C. R. Palevol 13 (2014) 569–585

Contents lists available at ScienceDirect

Comptes Rendus Palevol

www.sciencedirect.com

General Paleontology, Systematics and Evolution (Vertebrate Paleontology)

The scimitar-toothed cat *Machairodus aphanistus* (Carnivora: Felidae) in the Vallès-Penedès Basin (NE Iberian Peninsula)

Le chat à dents sabre Machairodus aphanistus *(Carnivora : Felidae) dans le bassin de Vallès-Penedès (Nord-Est de la péninsule Ibérique)*

Joan Madurell-Malapeira[a,b,*], Josep M. Robles[a,c], Isaac Casanovas-Vilar[a], Juan Abella[a,d], Pau Obradó[a], David M. Alba[a]

[a] *Institut Català de Paleontologia Miquel Crusafont, Universitat Autònoma de Barcelona, Edifici ICP-ICP, Carrer de les columnes s/n, Campus de la UAB, 08193 Cerdanyola del Vallès, Barcelona, Spain*
[b] *Dipartimento di Scienze della Terra, Sapienza Università di Roma, Piazzale Aldo Moro 5, 00185 Roma, Italy*
[c] *FOSSILIA Serveis Paleontològics i Geològics, S.L. c/Jaume I 87, 1er 5a, 08470 Sant Celoni, Barcelona, Spain*
[d] *Universidad Estatal Península de Santa Elena, Avda. principal, La Libertad, Santa Elena, Ecuador*

ARTICLE INFO

Article history:
Received 24 February 2014
Accepted after revision 20 May 2014
Available online 5 August 2014

Handled by Lars Vanden Hoek Ostende

Keywords:
Fossil cats
Machairodontinae
Late Miocene
Vallesian
Catalonia
Spain

ABSTRACT

Here, we revise all the published and unpublished scimitar-toothed cat remains from the Vallès-Penedès Basin (NE Iberian Peninsula), in order to confirm their taxonomic attribution to *Machairodus aphanistus* as well as to provide more precise information about its chronological distribution in this basin. The studied material (including dentognathic as well as postcranial remains) comes from the following localities: Can Mata indeterminate (late MN7+8 or MN9), Creu Conill 22 (MN9), Can Poncic 1 (MN9), Can Llobateres 1 (MN9), Santiga (MN9), La Tarumba 1 (MN10), Viladecavalls (MN10), Ronda Oest Sabadell ROS-D3 (MN10), and Torrent de Febulines (MN10). Most of the studied material fits well with the morphologic and metrical features characteristic of the Vallesian species *M. aphanistus*, with the exception of the remains from Creu Conill 22 (an undescribed partial P4 formerly attributed to this taxon), which belongs in fact to a medium-sized hyaenid. From a biostratigraphic viewpoint, the removal of the Creu Conill material from the hypodigm of *M. aphanistus* has important implications, because this locality (11.1 Ma) was considered to record the first appearance datum of this taxon in the Vallès-Penedès Basin. However, the report of a previously unpublished talus from Can Mata (late MN7+8 or MN9) indicates that this taxon was present in this basin at least by the earliest Vallesian. Therefore, our results indicate that the first appearance datum of *Machairodus* in the Vallès-Penedès Basin might be somewhat younger than previously assumed, although dating uncertainties for the Can Mata remains preclude a more precise assessment. In contrast, the new mandibular remains from ROS-D3 (MN10) are likely coeval with those from La Tarumba 1, with the last appearance datum of *M. aphanistus* in the Vallès-Penedès Basin corresponding to Torrent de Febulines (ca. 9.1 Ma). The postcranial material described from various Vallès-Penedès localities further indicates that *M. aphanistus* displayed less cursorial adaptations than its purported descendant *Homotherium*.

* Corresponding author.
E-mail address: joan.madurell@icp.cat (J. Madurell-Malapeira).

http://dx.doi.org/10.1016/j.crpv.2014.05.001
1631-0683/

Mots clés :
Félidés fossiles
Machairodontinae
Miocène supérieur
Vallésien
Catalogne
Espagne

RÉSUMÉ

Les auteurs présentent la révision de tous les restes (publiés ou non) de chats à dents-sabre du bassin de Vallès-Penedès (Nord-Est de la péninsule Ibérique), afin de confirmer leur attribution taxonomique à *Machairodus aphanistus*, et aussi de préciser la répartition chronologique de ce Félidé dans ce bassin. Le matériel étudié (qui comprend des restes dentaires et postcrâniens) provient des localités suivantes : Can Mata indéterminé (MN7+8 tardif ou MN9), Creu Conill 22 (MN9), Can Poncic 1 (MN9), Can Llobateres 1 (MN9), Santiga (MN9), La Tarumba 1 (MN10), Viladecavalls (MN10), Ronda Oest Sabadell ROS-D3 (MN10), et Torrent de Febulines (MN10). La plupart du matériel étudié correspond bien aux caractéristiques morphologiques et métriques, typiques de l'espèce vallésienne *Machairodus aphanistus*, à l'exception des restes de Creu Conill 22 (une P4 partielle, non décrite auparavant, attribuée à ce taxon), qui appartient en fait à un Hyaenidé de taille moyenne. Du point de vue biostratigraphique, l'élimination du matériel de Creu Conill de l'hypodigme de *M. aphanistus* a d'importantes implications biochronologiques, parce que cette localité (11,1 Ma) a été considérée comme ayant enregistré la première date d'apparition de ce taxon dans le bassin de Vallès-Penedès. Toutefois, un astragale inédit, recueilli à Can Mata (MN7+8 tardif ou MN9) indique que ce taxon était présent dans ce bassin au moins au début du Vallésien. Nos résultats indiquent donc que la première date d'apparition de *Machairodus* dans le bassin de Vallès-Penedès pourrait être un peu plus précoce qu'on ne l'estimait auparavant, bien que des incertitudes sur la datation des restes de Can Mata empêchent une évaluation plus précise. En revanche, les nouveaux restes mandibulaires de ROS-D3 (MN10) sont à peu près contemporains de ceux de La Tarumba 1, avec la dernière date d'apparition de *M. aphanistus* dans le bassin de Vallès-Penedès correspondant à Torrent de Febulines (ca. 9,1 Ma). Le matériel postcrânien décrit dans diverses localités du Vallès-Penedès indique, en outre, que *M. aphanistus* présente moins d'adaptations à la course que son descendant présumé *Homotherium*.

1. Introduction

1.1. The genus Machairodus

Machairodus Kaup, 1833 (Carnivora: Felidae: Machairodontinae) is an extinct genus of scimitar-toothed cats included in the tribe Machairodontini Gill, 1872 which also includes the genera *Amphimachairodus* Kretzoi, 1929 (formerly considered merely a subgenus of *Machairodus*), *Lokotunjailurus* Werdelin, 2003, *Xenosmilus* Martin et al., 1999 and *Homotherium* Fabrini, 1890. The earliest record of *Machairodus* apparently corresponds to *Machairodus robinsoni* Kurtén, 1976, from the Middle to Late Miocene of Bled Douarah in Tunisia (ca. 12.5–10 Ma; Geraads, 1989; Kurtén, 1976; Werdelin and Peigné, 2010), which is the only species of the genus currently recognized in Africa. The previously published (Geraads et al., 2002) African record of *M. aphanistus* (Kaup, 1832), which is the type species of the genus, is currently uncertain (Werdelin and Peigné, 2010). In turn, *Amphimachairodus kabir* (Peigné et al., 2005), originally described as a species of *Machairodus*, was recently reassigned to *Amphimachairodus* by Werdelin and Peigné (2010). For further discussion of the genus allocation of some African machairodontine species, see also Peigné et al. (2005), Sardella and Werdelin (2007), Werdelin (2003) and Werdelin and Sardella (2006).

Outside Africa, *Machairodus* is also recorded from North America and Eurasia. In North America, two different species may be recognized, ranging from the Late Miocene to the Early Pliocene (Antón et al., 2013; Martin, 1998): *M. catocopis* Cope, 1887 and *M. tanneri* Martin and Schultz, 1975. *Amphimachairodus coloradensis* (Cook, 1922), formerly attributed to *Machairodus*, was recently reassigned to the genus *Amphimachairodus* by Antón et al. (2013). In Eurasia, *only M. aphanistus* is generally recognized, being mostly recorded in the Vallesian (MN9–MN10), whereas Turolian (MN11–MN12) and Ventian (MN13) specimens are generally referred to *Amphimachairodus giganteus* (Wagner, 1848) (Antón et al., 2004; Beaumont, 1975; Montoya et al., 2006), although with some exceptions (see below). Additional species of *Machairodus* are however recognized by some authors (Peigné et al., 2005; Sotnikova, 1992), including *M. irtyschensis* Orlov, 1936 from the Early Pliocene of Pavlodar (Siberia; Orlov, 1936), *M. kurteni* Sotnikova, 1992 from the Ventian (MN13) of Kalmakpai (Kazakhstan; Sotnikova, 1992), and *M. horribilis* Schlosser, 1908 from China (Qiu et al., 2008). Based on their chronology, *M. kurteni* and *M. irtyschensis* might be alternatively attributable to *Amphimachairodus* and *Homotherium*, respectively. However, additional studies would be required to better ascertain their genus assignment. Therefore, we prefer to maintain tentatively the original attribution.

1.2. The European record of M. aphanistus

European remains of *M. aphanistus* outside the Iberian Peninsula are generally scarce and fragmentary. This species is mainly recorded from MN9 to MN10 localities, although there are some records from MN11; they include: Eppelsheim (MN9, type locality; Beaumont, 1975), Höwenegg (MN9; Bernor et al., 1988) and Dorn-Dürkheim

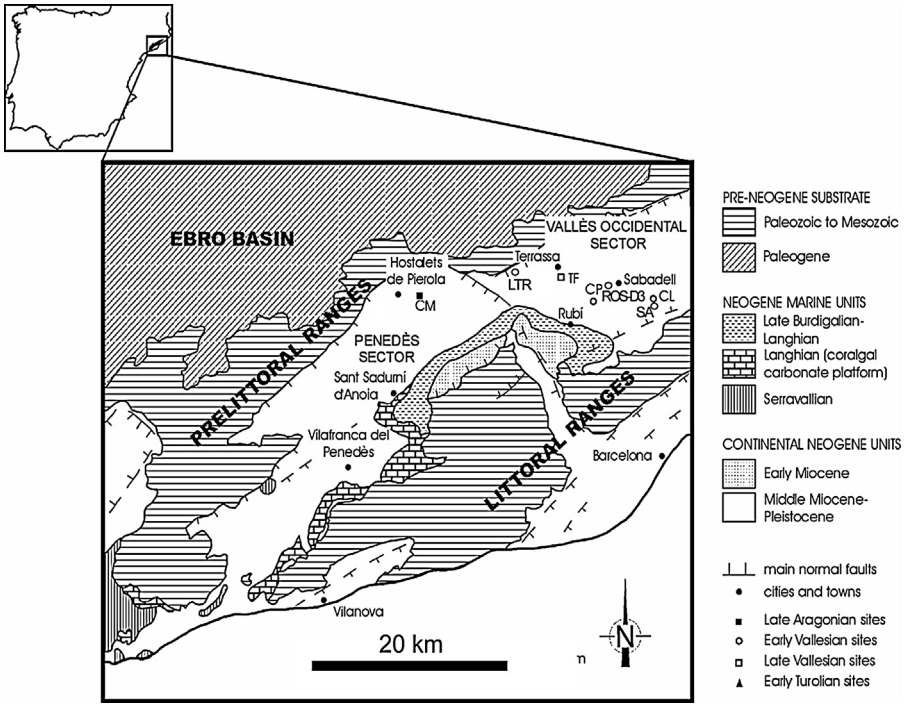

Fig. 1. Geographic map showing the location of the Vallès-Penedès Basin within the Iberian Peninsula (top left), and a schematic geologic map of this basin, showing the main geologic units and the paleontological sites with fossil remains of *Machairodus aphanistus*. Abbreviations: **CM**, Can Mata indeterminate; **CCN,** Creu Conill 22; **CLL**, Can Llobateres 1; **CP,** Can Poncic 1; **SA**, Santiga; **LTR**, La Tarumba 1; **ROS-D3**, Ronda Oest de Sabadell; **TF**, Torrent de Febulines.
Fig. 1. Carte géographique montrant la situation du bassin de Vallès-Penedès dans la péninsule Ibérique (en haut à gauche), et carte géologique schématique de ce bassin, montrant les principales unités géologiques ainsi que les sites paléontologiques avec des restes fossiles de *Machairodus aphanistus*. Abréviations: **CM**, Can Mata indeterminé ; **CCN,** Creu Conill 22 ; **CLL**, Can Llobateres 1 ; **CP,** Can Poncic 1 ; **SA**, Santiga ; **LTR**, La Tarumba 1 ; **ROS-D3**, Ronda Oest de Sabadell ; **TF**, Torrent de Febulines.

1 (MN11; Peigné et al., 2005) in Germany; Montredon and Soblay (MN10; Beaumont, 1975) in France; Charmoille (MN9; Beaumont, 1975) in Switzerland; Zillingdorf (MN9 or MN10; Beaumont, 1975; Peigné et al., 2005) in Austria; Csákvár (MN11; Morlo, 1997) in Hungary; Nessebar (MN9 or MN10; Spassov et al., 2006) in Bulgaria; and Kemiklitepe D (MN11; Bonis, 1994; Peigné et al., 2005; Spassov et al., 2006) and Mahmutgazi (MN11, Peigné et al., 2005) in Turkey.

In the Iberian Peninsula, *M. aphanistus* is recorded from several Spanish localities, including Los Valles de Fuentidueña (MN9, Duero Basin; Ginsburg et al., 1981), Batallones-1, 3 and 10 (MN10, Madrid Basin; Abella et al., 2011; Morales et al., 2008), and several Vallès-Penedès localities (Agustí et al., 1984, 1997; Alba et al., 2011a; Beaumont and Crusafont-Pairó, 1982; Crusafont and Truyols, 1954; Crusafont Pairó, 1959, 1964; Crusafont-Pairó and Golpe-Posse, 1972; Crusafont Pairó and Kurtén, 1976; Fraile et al., 1997; Golpe-Posse, 1974; Golpe-Posse et al., 1979; Pons-Moyà, 1990).

From older to younger, the previously known Vallès-Penedès localities are the following: Creu Conill 22, Can Poncic 1, Santiga and Can Llobateres 1, from MN9; and Torrent de Febulines and La Tarumba 1, from MN10. The remains from Los Valles de Fuentidueña were used to erect a distinct species, *M. alberdiae* Ginsburg et al., 1981, which is currently considered a subjective junior synonym of *M. aphanistus* (Peigné et al., 2005). The most abundant and complete remains of the species have been recovered from Batallones (Antón et al., 2004; Salesa et al., 2005; Turner et al., 2011).

The Iberian record of *M. aphanistus* in the Vallès-Penedès Basin (Fig. 1) is thus more restricted than in Europe as a whole, where this species persists into MN11, being apparently replaced by its purported descendant, *A. giganteus*, from MN11 onward. Here, we describe several unpublished remains of *M. aphanistus* from different localities of the Vallès-Penedès Basin, namely Can Mata (late MN7+8–MN9), Can Llobateres 1 (MN9), Viladecavalls (MN10) and Ronda Oest Sabadell ROS-D3 (MN10), further providing new data on the remains from the previously known localities of Can Poncic 1, Santiga, Can Llobateres 1, La Tarumba 1 and Torrent de Febulines. Finally, we discuss the presence of *M. aphanistus* in Creu Conill 22, putatively considered the first record of the *Hippotherium–Machairodus* association in the Iberian Peninsula (Agustí et al., 1997; Casanovas-Vilar et al., 2006).

2. Age and geological background

The Vallès-Penedès Basin is a small and elongated half-graben, parallel to the Catalan coastline and bounded by the Catalan Coastal Ranges. It originated during the extensional processes that resulted in the opening of the western Mediterranean in the Latest Oligocene (Bartrina et al., 1992; Cabrera et al., 1991, 2004; de Gibert and

Casanovas-Vilar, 2011; Roca and Guimerà, 1992). The stratigraphic record of the basin covers most of the Miocene, starting at the Ramblian (MN3) and ending by the Turolian (MN12), and besides some marine and transitional deposits that mainly correspond to the Langhian (early Middle Miocene), the infilling consists of continental sediments deposited in a context of alluvial fans (Agustí et al., 1985; Casanovas-Vilar et al., 2011b). The main alluvial fan systems were sourced from the southeastern reliefs during the Early Miocene and from the northwestern ones during the Middle and Late Miocene (Cabrera et al., 1991, 2004; de Gibert and Casanovas-Vilar, 2011). The basin has been intensively sampled for more than 70 years, and the Late Aragonian (Late Middle Miocene, MN7+8) and Vallesian (Late Miocene, MN9–MN10) records are particularly well known. More than 200 mammal-bearing sites are known from this interval, being placed in a detailed bio- and magnetostratigraphic framework, so that their age is well constrained (Agustí et al., 1985, 1997; Casanovas-Vilar et al., 2011a, b).

The studied specimens mostly come from well-sampled Vallesian sites of the basin. Creu Conill 22 is the oldest Vallesian site from the area, and it has been correlated by means of magnetostratigraphy to chron C5r.1n, which implies an age of ca. 11.1 Ma for the base of the Vallesian (Agustí et al., 1997; Garcés et al., 1996, 1997). The age of Can Llobateres 1, la Tarumba 1 and Torrent de Febulines is also well constrained, thanks to combined bio- and magnetostratigraphic data. Can Llobateres 1 correlates with the latest part of the Early Vallesian (MN9), yielding an age of 9.7 Ma (Agustí et al., 1997; Garcés et al., 1996). La Tarumba 1 would be slightly younger (ca. 9.6 Ma) and Torrent de Febulines would correspond to the last part of the Vallesian (ca. 9.1 Ma). The exact stratigraphic provenance of the Viladecavalls material is unknown, but the magnetostratigraphic data for the Viladecavalls section indicate that the series ranges from about 9.6 to 9.3 Ma (Agustí et al., 1997; Garcés et al., 1996). For Ronda Oest Sabadell (ROS), Santiga and Can Poncic 1, there are no magnetostratigraphic data, so their correlation is entirely based on biostratigraphy. Santiga and Can Poncic 1 have yielded abundant remains of the cricetid *Cricetulodon hartenbergeri*, characteristic of the *C. hartenbergeri* local range zone, which covers part of the Early Vallesian and ranges from about 10.4 to 9.9 Ma (Casanovas-Vilar et al., 2011a).

The Ronda Oest Sabadell locality ROS-D3 is here reported for the first time. All ROS localities were discovered as a result of paleontological work motivated by the construction in 2009–2011 of a road near the city of Sabadell (Blaya Martí et al., 2012). In the course of this work, several mammal-bearing sites were discovered and their stratigraphic position was accurately recorded. The preliminary study of the mammal succession (Blaya Martí et al., 2012; I.C.V. unpublished data) indicates that ROS sites range in age from the late Vallesian to the Early Turolian, i.e., from MN10 to MN11. Locality ROS-D3 is situated around 33 m of the 97 m-thick series of ROS sector D, and placed 13 m below locality ROS-D6 within the same sector. Given that no significant faults or hiatuses were detected in this particular series, the age of both sites is assumed to be roughly similar. ROS-D3 did not deliver any small mammal remains that would allow a correlation to the Vallès-Penedès local zones. In contrast, the rich rodent assemblage from ROS-D6 includes the murids *Progonomys cathalai* and *Parapodemus* sp. nov., together with the *cricetids Kowalskia ambarrensis* and *Rotundomys* cf. *montisrotundi*, the latter being represented by just two molars. The presence of murids, coupled with that of the cricetids *Kowalskia* and *Rotundomys*, indicate a late Vallesian (MN10) age. However, the rodent assemblage is very different from all those known from other MN10 localities of the same area, such as Viladecavalls and Torrent de Febulines. The abundance of murids and the rarity of *Rotundomys* are particularly conspicuous. *Rotundomys montisrotundi* ranges from about 9.6 to 9.3 Ma in the Vallès-Penedès, whereas *P. cathalai* and *Parapodemus* sp. nov. are not known from any other site (I.C.V., unpublished data). In the densely-sampled Teruel Basin (East-central Spain), *P. cathalai* first occurs at around 9.3 Ma, the first murid species recorded being *P. hispanicus* at 9.7 Ma (Van Dam et al., 2001). In the same area, *Parapodemus* does not occur until the Turolian. A similar situation is seen in the French record, even though *P. cathalai* may occur in older sites (Mein, 1999). Accordingly, ROS-D6 may correlate to the second half of the late Vallesian, being close in age to Trinxera Nord Autopista (ca. 9.3 Ma) and Torrent de Febulines (ca. 9.1 Ma). In support of this interpretation, *K. ambarrensis* is represented by scarce remains in these sites, and absent from older late Vallesian localities of the same basin (such as Viladecavalls and la Tarumba 1).

Finally, the exact stratigraphic provenance of the Can Mata material is unknown. The fossiliferous area of Can Mata is located near the town of els Hostalets de Pierola, with its Miocene outcrops recording the Middle to Late Miocene boundary. Traditionally, several loosely defined localities and isolated finds from this area were grouped into Hostalets Inferior (MN7+8) and Hostalets Superior (MN9) (Agustí et al., 1985; Golpe-Posse, 1974). More recently, many strictly defined localities have been recognized in this area, corresponding to the synthetic stratigraphic series of Can Mata (including both Abocador de Can Mata and Ecoparc de Can Mata), which range in age at least from the early MN7+8 to MN9 (Alba et al., 2006, 2011b; Casanovas-Vilar et al., 2011a; Moyà-Solà et al., 2009). Most of the old finds from Can Mata would be probably situated around the locality of Can Mata 1, which is considered to be latest Aragonian (ca. 11.2 Ma; Alba et al., 2011b; Casanovas-Vilar et al., 2011a), thus being either late MN7+8 or early MN9 in age. Therefore, it is likely that this find represents the oldest Vallès-Penedès occurrence of *Machairodus*, which has not been thus far recovered from the Late Aragonian (MN7+8) localities of the Abocador de Can Mata series (Alba et al., 2011b).

3. Material and methods

3.1. Abbreviations

Institutions and fossil collections: ICP, Institut Català de Paleontologia Miquel Crusafont, Universitat Autònoma de Barcelona; IPS, collections from the ICP.

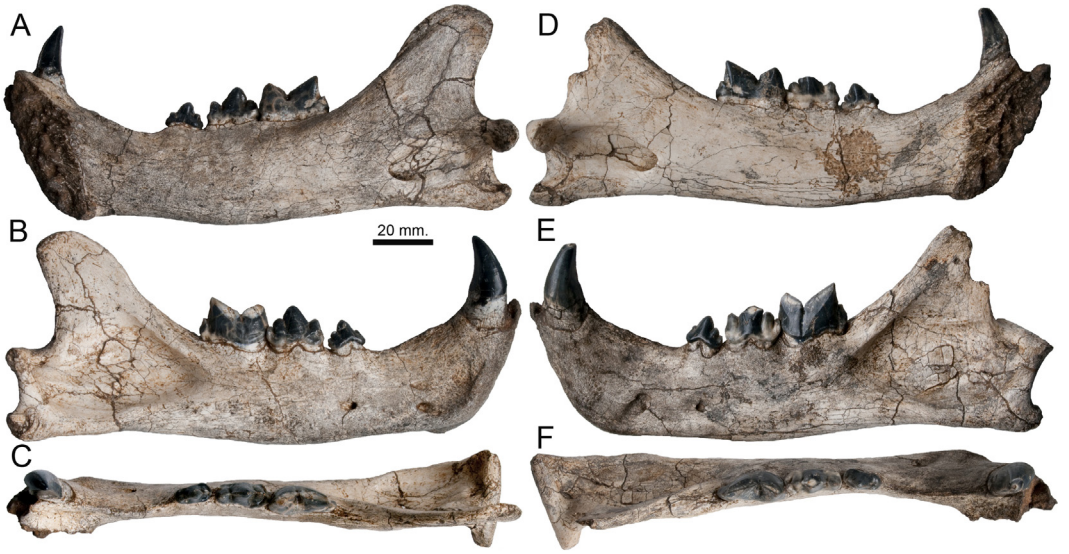

Fig. 2. (Color online.) Mandibular remains of *Machairodus aphanistus* from ROS-D3: **A–C**. Right hemimandible with c1–m1 IPS62083 in **A**: lingual; **B**: buccal; **C**: occlusal views. **D–F**. Left partial hemimandible with c1–m1 IPS62083 in **D**: lingual; **E**: buccal; **F**: occlusal views.
Fig. 2. (Couleur en ligne.) Restes mandibulaires de *Machairodus aphanistus* de ROS-D3 : **A–C**. Hémimandibule droite avec c1–m1 IPS62083 en vues **A** : linguale ; **B** : buccale ; **C** : occlusale. **D–F** : hémimandibule gauche partielle avec c1–m1 IPS62083 en vues **D** : linguale ; **E** : buccale ; **F** : occlusale.

Fossil sites: CM: Can Mata; CNN: Creu Conill; CP: Can Poncic 1; SA: Santiga; CLL: Can Llobateres; LTR: La Tarumba; VC: Viladecavalls; TF: Torrent de Febulines; ROS: Ronda Oest Sabadell.

3.2. Studied material, comparative sample and measurements

The fossil remains described in this paper (Figs. 2–6) are housed at the ICP. The comparative sample includes fossil remains of *M. aphanistus* from Los Valles de Fuentidueña housed at the ICP, as well as data from other Late Miocene European machairodontines based on data taken from the literature (Anton et al., 2004; Beaumont, 1975; Peigné et al., 2005; Salesa et al., 2012; Sardella and Werdelin, 2007; Sotnikova, 1992). Dental and mandibular measurements of the studied specimens were taken with a digital caliper to the nearest 0.1 mm.

4. Systematic paleontology

Order: CARNIVORA Bowdich, 1821
Suborder: FELIFORMIA Kretzoi, 1945
Family: FELIDAE Fischer, 1817
Subfamily: MACHAIRODONTINAE Gill, 1872
Genus *Machairodus* Kaup, 1833
Machairodus aphanistus (Kaup, 1832)
(Figs. 2–5)

4.1. Referred specimens

Can Mata: IPS30910, complete right talus.
Can Llobateres 1: IPS13169, complete left C1; IPS13178, crown fragment of right C1; IPS13166, complete left

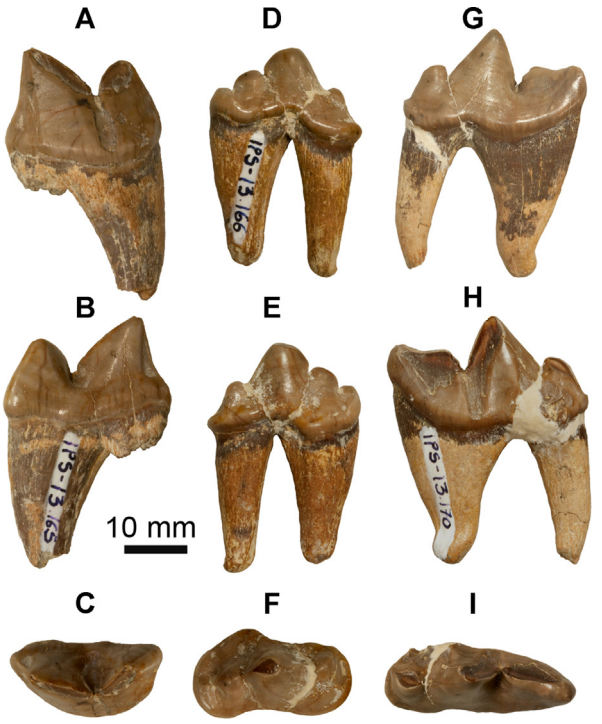

Fig. 3. (Color online.) Isolated dental remains of *Machairodus aphanistus* from the Vallès-Penedès Basin. **A–C**. Right m1 IPS13165 from CLL1 in **A**, buccal; **B**, lingual; **C**, occlusal views. **D–F**. Left P3 IPS13166 from Can Llobateres 1 in **D**, buccal; **E**, lingual; **F**, occlusal views. **G–H**. Right P4 IPS 13170 from Can Llobateres 1 in **G**, buccal; **H**, lingual; **I**, occlusal views.
Fig. 3. (Couleur en ligne.) Restes dentaires isolés de *Machairodus aphanistus* du bassin de Vallès-Penedès. **A–C**. m1 droite IPS13165 de CLL1 en vues **A**, buccale ; **B**, linguale ; **C**, occlusale. **D–F**. P3 gauche IPS13166 de CLL1 en vues **D**, buccale ; **E**, linguale ; **F**, occlusale. **G–H**. P4 droite IPS 13170 de CLL1 en vues **G**, buccale ; **H**, linguale ; **I**, occlusale.

Fig. 4. (Color online.) Isolated left P4 IPS28746 of Hyaenidae indet. from CCN22 previously attributed to *Machairodus aphanistus*. **A**, buccal; **B**, lingual; **C**, occlusal views.
Fig. 4. (Couleur en ligne.) P4 gauche isolée IPS28746 de Hyaenidae indet. de CCN22 précédemment attribuée à *Machairodus aphanistus*. Vues **A**, buccale ; **B**, linguale ; **C**, occlusale.

P3; IPS13164, complete left P4; IPS13170, right P4 lacking the protocone; IPS13168, right P4 lacking paracone and metacone; IPS15042, right P4 without parastyle and paracone; IPS15123, partial right P4; IPS13167, complete left p4; IPS13165, complete right m1; IPS15032, distal fragment of right m1; IPS15094, partial left scapula; IPS13176, complete right second metacarpal; IPS15045, proximal fragment of left second metacarpal; IPS15061, proximal fragment of right third metacarpal; IPS11381, left third metacarpal lacking the head; IPS13172, right fourth metacarpal; IPS15046, proximal fragment of left fifth metacarpal; IPS11020, right scapholunar; IPS11341, diaphysis of right femur; IPS13173, complete right third metatarsal; IPS15043, proximal fragment of right fourth metacarpal; IPS13174 and IPS13175, two complete right fifth metatarsals; IPS13171, right calcaneus; IPS15077, right navicular; IPS11183, left cuboid; IPS15021, IPS15022, IPS15015, and IPS15007, proximal phalanges; IPS15068, IPS15008, and IPS15017, middle phalanges.

Can Poncic 1: IPS15033, right premaxillary fragment with I2–I3; IPS13177, complete right p4.

Santiga: IPS13185, rostral fragment with left I1–M1 and right I1–M1.

Torrent de Febulines: IPS28929, two crown fragments of C1; IPS28932, left scapholunar; IPS28904, complete left fifth metatarsal.

Viladecavalls: IPS36058, proximal phalanx lacking the trochlea.

La Tarumba 1: IPS16286, right third metacarpal lacking the head.

Ronda Oest Sabadell ROS-D3: IPS62083, nearly complete left hemimandible with c1–m1 and associated complete right hemimandible with c1–m1.

4.2. Description and comparisons with unpublished material

Measurements: See Tables 1–3.

Upper teeth: The left P3 from CLL1 (IPS13166) displays a high protocone, slightly inclined lingually. The two accessory cusps are well-developed, the distal cusp being mesiodistally longer than the mesial cusp. A marked cingulum runs from the distal portion of the P3 crown to the protruding distolingual expansion, as in *Amphimachairodus* and *Panthera leo* (Antón et al., 2004; Fig. 3D–F), thus resembling the condition displayed by IPS13185 from SA (Beaumont and Crusafont-Pairó, 1982). IPS13166 differs from *Amphimachairodus* and *P. leo* in the concave buccal profile and the presence of a weak cingulum on the distolingual corner of the crown (Antón et al., 2004).

Mandible: The mandible from ROS-D3 (IPS62083) is long, with relatively deep and robust corpora, a relatively slender and moderately verticalized symphysis that is higher than the corpus, and a postcanine diastema longer (42.2–43.3 mm) than in other specimens of *M. aphanistus*, thus closely resembling those of *A. giganteus* (Antón et al., 2004; Sardella and Werdelin, 2007; Sotnikova, 1992). In the right hemimandible, there are three mental foramina, two below the diastema and another one below the p3 and close to the inferior margin of the mandible; on the left side, the two former foramina are more closely packed and partially fused with one another (Fig. 2B, E). The mandibular flange is only weakly developed, as it is characteristic of *M. aphanistus*, whereas in contrast *A. giganteus* has a better developed mandibular flange (Fig. 2B; Antón et al., 2004; Sardella and Werdelin, 2007). The corpus is thinner and shallower at the level of the distal portion of the diastema, and thickest and deepest at the level of the p4. The masseteric fossa is deep, reaching anteriorly the level of the m1 protoconid. The angular process is clearly individualized from the corpus and posterolingually projected. The coronoid process is rostrocaudally wide, posteriorly inclined and superiorly projecting well above the uppermost symphyseal level (Fig. 2A, D).

Lower teeth: Only the canines and cheek teeth are preserved in the mandible from ROS-D3 (IPS62083). All these teeth are completely preserved, except for the missing tip of the right c1. The cheek teeth display a moderate degree

Fig. 5. (Color online.) Postcranial remains of *Machairodus aphanistus* from the Vallès-Penedès Basin. **A–E**. Right metatarsal V IPS13174 from CLL1 in **A**, dorsal; **B**, medial; **C**, plantar; **D**, lateral; **E**, proximal views. **F–J**. Left metatarsal V IPS28904 from TF in **F**, dorsal; **G**, lateral; **H**, plantar; **I**, medial; **J**, proximal views. **K–O**. Right metacarpal III IPS16286 from LTR in **K**, dorsal; **L**, medial; **M**, palmar; **N**, lateral; **O**, proximal views. **P–T**, Right metacarpal II IPS13176 from CLL1 in **P**, dorsal; **Q**, medial; **R**, palmar; **S**, lateral; **T**, proximal views. **U–Y**. Left metacarpal III IPS11381 from CLL1 in **U**, dorsal; **V**, lateral; **W**, palmar; **X**, medial; **Y**, proximal views. **Z–D′**, Partial right metatarsal IV IPS15043 from CLL1 in **Z**, dorsal; **A′**, medial; **B′**, plantar; **C′**, lateral, **D′**, proximal views. **E′–I′**. Proximal fragment of left fifth metacarpal IPS15046 from CLL1 in **E′**, dorsal; **F′**, medial; **G′**, palmar; **H′**, lateral; **I′**, proximal views.

Fig. 5. (Couleur en ligne.) Restes postcrâniens de *Machairodus aphanistus* du bassin de Vallès-Penedès. **A–E**. Métatarsien V droit IPS13174 de CLL1 en vues **A**, dorsale ; **B**, médiale ; **C**, plantaire ; **D**, latérale ; **E**, proximale. **F–J**. Métatarsien V gauche IPS28904 de TF en vues **F**, dorsale ; **G**, latérale ; **H**, plantaire ; **I**, médiale ; **J**, proximale. **K–O**. Métacarpien III droit IPS16286 de LTR en vues **K**, dorsale ; **L**, médiale ; **M**, palmaire ; **N**, latérale ; **O**, proximale. **P–T**. Métacarpien II droit IPS13176 de CLL1 en vues **P**, dorsale ; **Q**, médiale ; **R**, palmaire ; **S**, latérale ; **T**, proximale. **U–Y**. Métacarpien III gauche IPS11381 de CLL1 en vues **U**, dorsale ; **V**, latérale ; **W**, palmaire ; **X**, médiale ; **Y**, proximale. **Z–D′**. Métatarsien IV droit IPS15043 de CLL1 en vues **Z**, dorsale ; **A′**, médiale ; **B′**, plantaire ; **C′**, latérale ; **D′**, proximale. **E′–I′**. Fragment proximal du 5^{e} métacarpien gauche IPS15046 de CLL1 en vues **E′**, dorsale ; **F′**, médiale ; **G′**, palmaire ; **H′**, latérale ; **I′**, proximale.

Table 1
Measurements (in mm) of the upper dentition of *Machairodus aphanistus* from the Vallès-Penedès Basin.
Tableau 1
Mensurations (en mm) de la dentition supérieure de *Machairodus aphanistus* du bassin de Vallès-Penedès.

		C1			P3		P4					M1	
Catalog No.	Site	L	W	H	L	W	L	W	Lps	Lpa	Lme	L	W
IPS13185	SA	24.2	14.1	62.0	23.1	12.9	36.9	18.2	11.4	13.9	14.3	7.0	11.3
IPS13185	SA	24.3	14.7	65.6	21.6	13.9	36.8	21.3	10.3	13.5	14.1	7.9	15.1
IPS13169	CLL1	23.1	12.2	50.0									
IPS13178	CLL1	26.8	13.9										
IPS13166	CLL1				22.2	11.8							
IPS13170	CLL1						33.2		9.1	12.6	11.9		
IPS13164	CLL1						32.9	15.3	8.3	13.2	12.8		
IPS13168	CLL1							15.1	8.2				
IPS15123	CLL1										12.1		
IPS15042	CLL1									12.1	14.1		
IPS28929	TF	30.2	13.7										

L: mesiodistal length; W: labiolingual breadth; H: crown height; Lps: mesiodistal length of P4 parastyle; Lpa: mesiodistal length of P4 paracone; Lme: mesiodistal length of P4 metastyle. See Materials and methods for locality abbreviations.
L, longueur mésiodistale ; W, largeur labiolinguale ; H, hauteur de la couronne ; Lps, longueur mésiodistale du parastyle P4 ; Lpa, longueur mésiodistale du paracône P4 ; Lme, longueur mésiodistale du métastyle P4. Voir Materials and methods pour les abréviations de localités.

of wear, with dentine exposure in both m1 and in the protoconid of the left p4 (Fig. 2B, E). c1 is high-crowned, proportionally larger than in *A. giganteus*, and implanted obliquely relative to the postcanine tooth row. The crown displays an oval (longer than broad) occlusal profile and is tilted distally (with its apex almost reaching the distalmost level of the crown base). The crown may be divided into a markedly convex buccal portion and a slightly concave distolingual portion. The latter is delimited by two (distal and mesiolingual) serrated crests that run from cervix to the apex. The mesiolingual crest is thicker than the distal one, and, unlike the latter, it ends shortly before reaching the crown apex; next to the former there is mesial shallow sulcus that runs from the cervix to about crown mid-height (Fig. 2A, B).

The premolars are tricuspid and somewhat broader distally than mesially. p3 displays a low and finely-serrated protoconid that is slightly tilted distalwards, well-developed mesial and distal accessory cuspids (the mesial one slightly smaller and more lingually situated than the distal one), and a distinct distal cingulid (Fig. 2C). p4 displays a similar morphology but is much larger than the preceding premolar. The protoconid has a similar occlusal morphology, although it is much higher, the mesial and distal accessory cuspids are comparatively better developed and similar in size to one another (being as high as the p3 protoconid), and the distal cingulid is even more conspicuous. As compared with the p4 from CLL1 (IPS13167) and CP (IPS13177), the p4 from ROS-D3 shows better developed and higher accessory cuspids and a stronger distal cingulid, thus more closely resembling the condition observed in *A. giganteus* than the previously described specimens (Beaumont and Crusafont-Pairó, 1982; Geraads et al., 2004; Salesa et al., 2012).

Table 2
Measurements (in mm) of the lower dentition and mandible of *Machairodus aphanistus* from the Vallès-Penedès Basin.
Tableau 2
Mensurations (en mm) de la dentition inférieure et de la mandibule de *Machairodus aphanistus* du bassin de Vallès-Penedès.

			c1			p3		p4		m1				
Catalog No.	Laterality	Locality	L	W	H	L	W	L	W	L	W	Lpa	Lpr	Lt
IPS62083	Left	ROS-D3	17.8	11.1	25.5	15.6	7.8	23.2	10.5	27.7	12.1	13.9	14.4	5.2
IPS62083	Right	ROS-D3	16.8	11.2	27.4	15.5	8.1	23.0	10.4	27.9	12.3	14.7	13.4	4.8
IPS13167	Left	CLL1						21.5	9.9					
IPS13177	Right	CP1						22.3	10.4					
IPS13165	Right	CLL1								26.5	12.5	13.3	12.9	3.2
IPS15032	Right	CLL1									12.5			

Catalog No.		Locality	Ld	Lm	LSD	Hp4	Hm1	Hd	Hr	Hs
IPS62083	Left	ROS-D3	43.3	211.8	66.4	41.6	41.4	35.0		65.3
IPS62083	Right	ROS-D3	42.2	208.5	66.3	40.1	41.1	35.4	84.6	64.3

L: mesiodistal length; W: labiolingual breadth; H: crown height; Lpa: mesiodistal length of m1 paraconid; Lpr: mesiodistal length of m1 protoconid; Lt: mesiodistal length of m1 talonid; Ld: mesiodistal length of the diastema; Lm: maximum mandibular length; LSD: mesiodistal length of the postcanine tooth row; Hp4: mandibular corpus height at p4; Hm1: mandibular corpus height at m1; Hd: mandibular corpus height at the diastema; Hr: maximum mandibular ramus height; Hs: maximum symphysis height. See Materials and methodsfor locality abbreviations.
L, longueur mésiodistale ; W, largeur labiolinguale ; H, hauteur de la couronne ; Lpa, longueur mésiodistale du paraconide m1 ; Lpr, longueur mésiodistale du protoconide m1; Lt, longueur mésiodistale du talonide m1 ; Ld, longueur mésiodistale du diastème ; Lm, longueur mandibulaire maximale ; LSD, longueur mésiodistale de la rangée de dents postcanines ; Hp4, hauteur du corps mandibulaire à la p4 ; Hm1, hauteur du corps mandibulaire à la m1 ; Hd, hauteur du corps mandibulaire au diastème ; Hr, hauteur maximale du ramus mandibulaire ; Hs, hauteur maximale de la symphyse. Voir Materials and methods pour les abréviations de localités.

Table 3
Measurements (in mm) of the postcranial remains of *Machairodus aphanistus* from the Vallès-Penedès Basin.
Tableau 3
Mensurations (en mm) des restes postcrâniens de *Machairodus aphanistus* du bassin de Vallès-Penedès.

Catalog No.	Element	Locality	L	PMLD	MMLD	DMLD	PDPD	MDPD	DDPD	APG	MLG	MLD	MLDp	MLDd	Hm	Hl	DPD	PDD
IPS15094	Scapula	CLL1								44.7	34.6							
IPS11020	Scapholunar	CLL1										43.8					36.9	26.1
IPS28932	Scapholunar	TF										49.1					39.4	27.6
IPS13176	Metacarpal II	CLL1	93.7	23.1	14.4	19.3	24.3	13.7	15.2									
IPS15045	Metacarpal II	CLL1		21.2			23.7											
IPS11381	Metacarpal III	CLL1		20.2	13.1		20.5	11.5										
IPS15061	Metacarpal III	CLL1		19.6			20.8											
IPS16286	Metacarpal III	LTR		22.8	13.1		25.5	11.3										
IPS13172	Metacarpal IV	CLL1	102.3	16.9	12.3	17.2	19.3	11.8	17.6									
IPS15046	Metacarpal V	CLL1		19.9	13.4		21.2	12.0										
IPS11341	Femur	CLL1			29.4			25.8										
IPS30901	Talus	CM											51.2		53.8	39.2		
IPS13171	Calcaneus	CLL1											24.4	30.5	95	87.9		
IPS15077	Navicular	CLL1										25.1					34.7	17.0
IPS11183	Cuboid	CLL1										25.6					31.3	28.8
IPS13173	Metatarsal III	CLL1	131	25.7	17.9	24.5		15.6	23.4									
IPS15043	Metatarsal IV	CLL1		18.0	13.2		21.7	13.1										
IPS13175	Metatarsal V	CLL1	110.0	18.7	10.3	16.3	14.8	11.0	16.6									
IPS13174	Metatarsal V	CLL1	104.9	20.4	9.6	16.7	16.8	10.6	16.2									
IPS28904	Metatarsal V	TF	114.4	23.11	11.0	19	22.3	12.9	19.5									
IPS36058	Proximal phalanx	VC		18.7	14.7		16.4	10.2										
IPS15007	Proximal phalanx	CLL1	39.2	19.2	12.8	14.4	14.4	10.7	10.6									
IPS15015	Proximal phalanx	CLL1	47.3	20.6	13.9	15.1	17.7	10.9	12.1									
IPS15021	Proximal phalanx	CLL1	46.8	20.4	13.9	15.3	16.1	10.8	11.8									
IPS15022	Proximal phalanx	CLL1	39.7	17.8	12.9	15.5	15.5	11.3	10.5									
IPS15068	Middle phalanx	CLL1	33.3	16.5		14.3	14.1		11.2									
IPS15017	Middle phalanx	CLL1	30.7	17.2		14.9	14.2		10.1									
IPS15008	Middle phalanx	CLL1	35.4	16.6		15.0	14.3		11.4									

L: proximodistal length; PMLD: proximal mediolateral width; MMLD: mediolateral width at midshaft; DMLD: distal mediolateral width; PDPD: proximal dorsopalmar height; MDPD: dorsopalmar width at midshaft; DDPD: distal dorsopalmar height; APG: anteroposterior diameter of the glenoid cavity; MLG: mediolaterial diameter of the glenoid cavity; MLD: maximum mediolateral diameter; MLDp: proximal maximum mediolateral diameter; MLDd: distal maximum mediolateral diameter; Hm: medial height; Hl: lateral height; DPD: maximum dorsopalmar height; PDD: maximum proximodistal length.
L, longueur proximodistale ; PMLD, largeur proximale médiolatérale ; MMLD, largeur médiolatérale au milieu ; DMLD, largeur médiolatérale distale ; PDPD, hauteur proximale dorsopalmaire ; MDPD, largeur dorsopalmaire au milieu ; DDPD, hauteur dorsopalmaire distale ; APG, diamètre antéroposterieur de la cavité glénoïde ; MLG, diamètre médiolatéral de la cavité glénoïde ; MLD, diamètre médiolatéral maximal ; MLDp, diamètre médiolatéral maximal proximal ; MLDd, diamètre médiolatéral maximal distal ; Hm, hauteur médiale ; Hl, hauteur latérale ; DPD, hauteur maximale dorsopalmaire ; PDD, longueur maximale proximodistale.

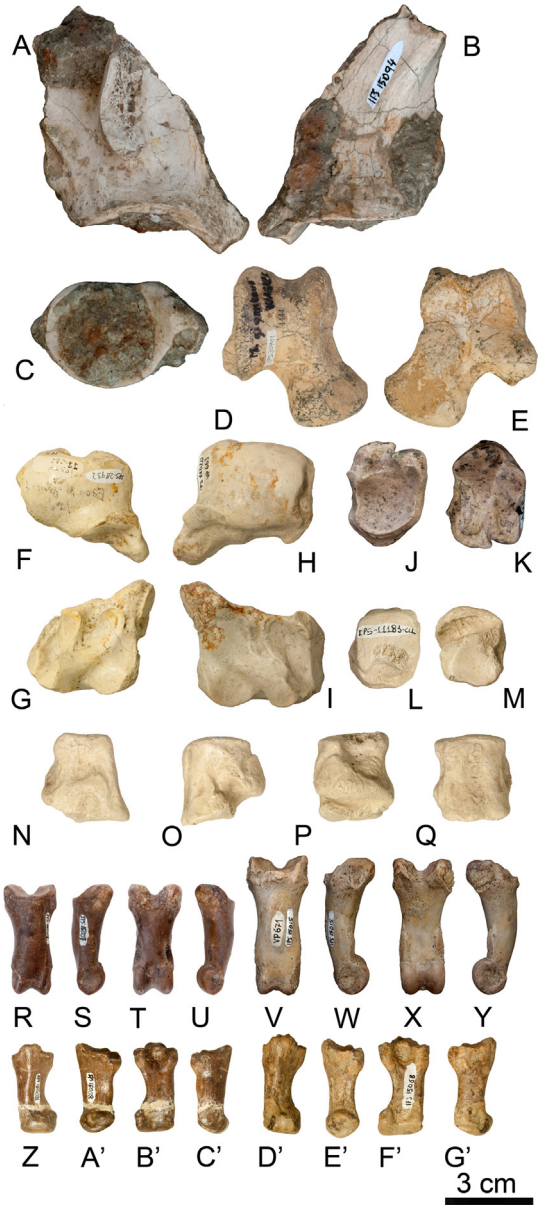

Fig. 6. (Color online.) Postcranial remains of *Machairodus aphanistus* from the Vallès-Penedès Basin. **A– C**. Partial left scapula IPS15094 from CLL1 in **A**, lateral; **B**, medial; **C**, distal views. **D–E**. Right talus IPS30901 from CM in **D**, dorsal; **E**, plantar views. **F–G**. Left scapholunar IPS28932 from TF in **F**, proximal; **G**, distal views. **H–I**. Right scapholunar IPS11020 from CLL1 in **H**, proximal; **I**, distal views. **J–K**. Right navicular IPS15077 from CLL1 in **J**, dorsal; **K**, plantar views. **L–Q**. Left cuboid IPS11183 from CLL1 in **L**, lateral; **M**, medial; **N**, proximal; **O**, plantar, **P**, distal; **Q**, dorsal views. **R–U**. Proximal phalanx IPS15007 from CLL1 in **R**, dorsal; **S,U,** lateral/medial; **T**, volar views. **V–Y**. Proximal phalanx IPS15015 from CLL1 in **V**, dorsal; **W, Y**, lateral/medial; **X**, volar views. **Z–C′**. Middle phalanx IPS15008 from CLL1 in **Z**, dorsal; **A′, C′**, lateral/medial; **B′**, volar views. **D′–G′**, middle phalanx IPS15068 from CLL1 in **D′**, dorsal; **E′, G′**, lateral/medial; **F′**, volar views.

Fig. 6. (Couleur en ligne.) Restes postcrâniens de *Machairodus aphanistus* du bassin de Vallès-Penedès. **A–C**. Scapula gauche partielle IPS15094 de CLL1 en vues **A**, latérale ; **B**, médiale ; **C**, distale. **D–E**. Astragale droit IPS30901 de CM en vues **D**, dorsale ; **E**, plantaire. **F–G**. Scapholunaire gauche IPS28932 de TF en vues **F**, proximale ; **G**, distale. **H–I**. Scapholunaire droit IPS11020 de CLL1 en vues **H**, proximale ; **I**, distale. **J–K**. Naviculaire droit IPS15077 de CLL1 en vues **J**, dorsale ; **K**, plantaire. **L–Q**. Cuboïde gauche IPS11183 de CLL1 en vues **L**, latérale ; **M**, médiale ; **N**, proximale ; **O**, plantaire, **P**, distale ; **Q**, dorsale. **R–U**. Phalange proximale IPS15007 de CLL1 en vues **R**, dorsale ; **S,U,** latérale/médiale ; **T**, volaire. **V–Y**. Phalange proximale IPS15015 de CLL1 en vues **V**, dorsale ; **W, Y**, latérale/médiale ; **X**, volaire. **Z–C′**, phalange moyenne IPS15008 de CLL1 en vues **Z**, dorsale ; **A′, C′**, latérale/médiale ; **B′**, volaire. **D′–G′**, phalange moyenne IPS15068 de CLL1 en vues **D′**, dorsale ; **E′,G′**, latérale/médiale ; **F′**, volaire.

The lower carnassial (m1) displays two main cuspids, the paraconid being lower and mesiodistally shorter than the protoconid, which is markedly asymmetrical (very tilted distally). The m1 further displays a short but distinct talonid with a distinct metaconid (Fig. 2C), which is relatively well-developed as compared with other specimens of *M. aphanistus* (Antón et al., 2004). Another m1 is available from CLL1 (IPS13165). It displays a similar occlusal morphology as the carnassials from the ROS-D3 mandible (IPS62083), although that from CLL1 displays a less developed talonid that further lacks a distinct metaconid (Fig. 3A–C).

Scapula: A partial right scapula (distal fragment) from CLL1 (IPS15094; Fig. 4A–C) preserves the glenoid cavity, the neck and the supraglenoid tuberosity. The glenoid cavity displays a subcircular profile as in *Smilodon fatalis* and *Homotherium latidens* from Europe, thus differing from *H. serum*, *H. ischyrus* and extant large felids, which display a transversely wider cavity that is rather ovoid (Ballesio, 1963; Martin et al., 2011; Merriam and Stock, 1932; Rawn-Schatzinger, 1992). The supraglenoid tuberosity is mediolaterally wider than in *Homotherium*, thus resembling the condition observed in extant *P. leo*.

Carpus: One scapholunar from CLL1 (IPS11020; Fig. 4H, I) shares several characters with *Homotherium*. The radial facet is clearly convex and narrower than in extant large felids and *Smilodon*, thus being more similar to the condition seen in *Homotherium*. The proximal process is palmomedially situated, whereas in extant large felids and *Homotherium*, this process is more palmarly projected, and in *Smilodon*, it is clearly projected medially. The facet for the radial sesamoid is large and rounded, as in *Homotherium* (Ballesio, 1963; Hearst et al., 2011; Martin et al., 2011; Merriam and Stock, 1932; Rawn-Schatzinger, 1992). The scapholunar has a distal rectangular outline, with the facet for the radial sesamoid oriented along the dorsoplantar plane. The facet for the trapezoid, situated on the dorsomedial corner of the bone, is triangular and slightly convex, being separated from the facet for the trapezium by a narrow dorsopalmar ridge. The facet for the trapezium extends towards the palmar margin, as in *Homotherium* and *P. leo*, but unlike in *Smilodon* (Ballesio, 1963; Hearst et al., 2011; Merriam and Stock, 1932; Rawn-Schatzinger, 1992). The facet for the magnum is very concave, running from the palmar to the dorsal side. The facet for the unciform is rectangular and narrower than in extant large felids and *Homotherium*, thus being similar to the condition displayed by *Smilodon* (Ballesio, 1963; Hearst et al., 2011; Merriam and Stock, 1932; Rawn-Schatzinger, 1992). The scapholunar from CLL1 (IPS11020) displays the same morphological features as that previously published from TF (IPS28932;

Fig. 4F, G; Pons-Moyà, 1990), although the latter is somewhat larger in size (Table 3).

Metacarpus: There are two second metacarpals available from CLL1: IPS13176 (Fig. 5P–T), which is complete; and IPS15045, which only preserves the proximal portion. IPS13176 is stouter (proximodistally shorter and mediolaterally wider) than in *Homotherium*, *Smilodon* and *P. leo*, thus more closely resembling the condition of *Xenosmilus* (Fig. 8). The diaphysis is slightly curved palmarly, as in *P. atrox* but unlike in the other taxa mentioned above (Ballesio, 1963; Martin et al., 2011; Merriam and Stock, 1932; Rawn-Schatzinger, 1992). The base displays a triangular proximal profile, as in *Homotherium*, *Smilodon* and extant large felids (Christiansen and Adifssen, 2007; Merriam and Stock, 1932; Rawn-Schatzinger, 1992). The articular facet for the trapezoid is markedly concave, as in extant large felids, *Megantereon* and *Smilodon*, thus differing from the flat facet displayed by *Homotherium* (Ballesio, 1963; Christiansen and Adolfssen, 2007; Merriam and Stock, 1932; Rawn-Schatzinger, 1992). The facet for the trapezium is triangular and relatively small, as in *Homotherium*, whereas in *Xenosmilus* it is more circular and in *Smilodon* larger and more elongated (Ballesio, 1963; Martin et al., 2011; Merriam and Stock, 1932; Rawn-Schatzinger, 1992). The articular facets for the magnum, present on the lateral side of the metacarpal base, are poorly preserved in the two available specimens. The articular facet for the third metacarpal is very conspicuous and distally-projected, similar to the morphology displayed by extant large felids and *Homotherium*.

The third metacarpal is represented by three specimens: IPS11381 from CLL1 (Fig. 5U–Y) is complete, whereas IPS15061 from CLL1 and IPS16286 from LTR (Fig. 5K–O) only preserve the proximal portion. The base is poorly preserved in all the available specimens, although it can be discerned that the facet for the magnum is concave, as in *Xenosmilus*, *Megantereon* and *Smilodon*, whereas in contrast the facet for the magnum is convex, as in *Homotherium* and *Panthera* (Christiansen and Adolfssen, 2007; Martin et al., 2011; Rawn-Schatzinger, 1992). The proximolateral facet for the unciform is posteriorly elongated and less triangular than in *P. leo*, thus resembling the morphology displayed by *Homotherium*, *Meganteron* and *Xenosmilus* (Christiansen and Adolfssen, 2007; Martin et al., 2011; Rawn-Schatzinger, 1992). The dorsalmedial facet for the second metacarpal is dorsodistally elongated compared to *Homotherium*, *Megantereon* and *Xenosmilus*, thus resembling the condition displayed by *P. leo* (Ballesio, 1963; Christiansen and Adolfssen, 2007; Martin et al., 2011, Rawn-Schatzinger, 1992). The diaphysis is slender (mediolaterally narrow relative to length) and subtriangular in cross-section.

A proximal fragment of a fifth metacarpal from CLL1 (IPS15046; Fig. 5E′–I′) shows that the facet for the unciform is rectangular and very convex, thus being similar in shape but less posteromedially inclined than in *Homotherium*, and more clearly differing from the triangular morphology displayed by *Smilodon, P. atrox* and extant *P. leo* (Ballesio, 1963; Merriam and Stock, 1932; Rawn-Schatzinger, 1992). The medial articular tubercle for the fourth metacarpal is less developed than in extant large felids and *P. atrox*, thus resembling the condition seen in *Smilodon* and *Homotherium* (Merriam and Stock, 1932; Rawn-Schatzinger, 1992). The proximolateral tuberosity is flattened or depressed, as in *Smilodon* and *Homotherium*, whereas in extant large cats and *P. atrox* it is generally convex (Merriam and Stock, 1932; Rawn-Schatzinger, 1992).

Tarsus: The right talus from CM (IPS30901; Fig. 4D, E) is complete and well preserved. The trochlea is grooved and shallower than in extant large felids, thus resembling the condition observed in *Homotherium*, *Amphimachairodus* and *Smilodon*. In contrast, the neck is relatively longer than in *Homotherium*, *Amphimachairodus*, *Smilodon* and *P. leo* (Ballesio, 1963; Berta, 1987; Merriam and Stock, 1932; Salesa et al., 2012). On the plantar side, the astragalar foramen can be discerned, although it is poorly preserved. The sustentacular and navicular facets are also poorly preserved, being separated by a deep and wide groove from the rectangular (mediolaterally wide) and strongly convex astragalocalcanear facet, resembling the morphology of the various species of *Homotherium* (Ballesio, 1963; Berta, 1987; Merriam and Stock, 1932).

A right navicular from CLL1 (IPS15077; Fig. 4J–K) shows that the astragalar facet is rounded and slightly concave, as in other Machairodontini. The ectocuneiform facet is slightly larger than the mesocuneiform facet, further being merely separated from one another dorsally by a ridge as in *Smilodon* and *Homotherium*. The cuboid and calcaneal facets are contiguous but separated by a weak ridge, as in *Smilodon* and *Homotherium* (Ballesio, 1963; Berta, 1987; Martin et al., 2011; Merriam and Stock, 1932). The morphology of the described specimen fits perfectly with that previously reported for the same element from Los Valles de Fuentidueña (IPS12664; Crusafont-Pairó and Ginsburg, 1973).

The left cuboid from CLL1 (IPS11183; Fig. 4L–Q) similarly shows the same morphology displayed by the specimen from Los Valles de Fuentidueña (IPS12661) reported by Crusafont-Pairó and Ginsburg (1973). The calcaneal proximal facet is quadrangular and slightly convex, thus differing from the more rectangular and flat morphology displayed by *Homotherium*. IPS11183 is proximodistally higher than in *Homotherium* and *Smilodon*, more closely approaching the condition observed in extant large felids (Martin et al., 2011; Merriam and Stock, 1932; Rawn-Schatzinger, 1992). The ectocuneiform facet is dorsoventrally high and located more dorsally than in *Homotherium*. The small and triangular navicular facet is located on the dorsodistal corner of the bone, like in *Homotherium*. In lateral view, the oblique, deep and wide groove for the insertion of the m. peroneus longus is more marked and deeper than in the specimen from Los Valles de Fuentidueña (Crusafont-Pairó and Ginsburg, 1973), thus more closely approaching the condition of *Homotherium* (Martin et al., 2011). The facets for the fourth and fifth metatarsals are visible on the distal portion of the bone, although poorly preserved.

Metatarsus: A proximal fragment of fourth metatarsal from CLL1 (IPS15043, Fig. 5Z–D″) shows that the proximal facet for the cuboid is rectangular and slightly convex, further being mediolaterally broader on its plantar than on

its dorsal portion, as in other Machairodontini, but unlike in pantherines (Martin et al., 2011; Rawn-Schatzinger, 1992). There is only a single, deep and distally-projected facet for the fifth metatarsal, whereas in *Homotherium*, *Smilodon*, *Amphimachairodus* and pantherines there are two deep but less distally-projected facets (Ballesio, 1963; Berta, 1987; Merriam and Stock, 1932; Rawn-Schatzinger, 1992; Salesa et al., 2012). The fourth metatarsal displays two medial facets for the third metatarsal: a subcircular one, situated dorsoproximally; and a more rectangular and inclined one, situated more palmarly. The circular dorsal facet is generally situated more proximally in *Homotherium*, *Smilodon* and *P. leo* than in the studied specimen, whereas the posterior facet in the latter resembles that observed in *P. leo* (Ballesio, 1963; Berta, 1987; Merriam and Stock, 1932; Rawn-Schatzinger, 1992). Three fifth metatarsals are available: one from CLL1 (IPS13175) published by Beaumont and Crusafont-Pairó (1982), another from TF (IPS28904, Fig. 5F–J) published by Golpe-Posse et al. (1979) and Pons-Moyà (1990), and a third one CLL1 (IPS13174, Fig. 5A–E) that remained unpublished. All these specimens display the morphology already described by Beaumont and Crusafont-Pairó (1982) and Pons-Moyà (1990), although that from TF is comparatively stouter and further displays a very deep ligamental groove on its proximoplantar portion that is not observed in the specimens from CLL1 (Fig. 8).

Phalanges: Four complete proximal phalanges from CLL1 (IPS15015, IPS15007, IPS15022 and IPS15021; Fig. 4R–Y) and a proximal fragment from VC (IPS36058) are available. Their comparison with extant *P. leo* and the extinct *H. latidens* specimens do not enable their attribution to either the manus or the pes, or to any specific ray. These specimens display the same morphology as that previously described from Los Valles de Fuentidueña (IPS12667; Crusafont-Pairó and Ginsburg, 1973), being characterized by a mediolaterally robust diaphysis, a vertically oriented proximal articular surface and a deep ligamental groove on its proximal portion, and thus resembling the morphology displayed by *Amphimachairodus*, *Homotherium* and *Smilodon* (Ballesio, 1963; Berta, 1987; Gaudry, 1832; Merriam and Stock, 1932; Salesa et al., 2012).

The comparison of three middle phalanges from CLL1 (IPS15068, IPS15008 and IPS15017; Fig. 4A–H) with those of pantherines and *H. latidens* do not allow us to provide with an anatomical attribution to either manual or pedal phalanges. IPS15068 (Fig. 4E–H) and IPS15008 (Fig. 4A–D) have slender and longer shafts than in IPS15017. In general terms, the reported middle phalanges seem slightly stouter than those of *P. leo*. The same elements of *Homotherium* and *Smilodon* seem generally slenderer and proximodistally shorter (Ballesio, 1963; Berta, 1987; Merriam and Stock, 1932).

5. Discussion

5.1. Taxonomic attribution

Creu Conill: Agustí et al. (1997) reported the presence of *M. aphanistus* from CCN22 (MN9; 11.1 Ma) on the basis of an undescribed left P4 (IPS28746; Fig. 6A–C). In fact, the morphology of this P4, which does not preserve the protocone, is quite different from those of *M. aphanistus*. The parastyle in IPS28746 lacks the well-developed buccal cingulum that is characteristic of *M. aphanistus*, and which can be observed in the P4 of this taxon available from the Vallès-Penedès Basin from CLL1 (IPS13170; Fig. 3G–I) and SA (IPS13185). Moreover, IPS28746 from CCN22 displays a slightly marked lingual cingulum running from the distal aspect of the metacone to the mesial portion of the paracone (Fig. 6B), which cannot be observed in the Vallès-Penedès material of *M. aphanistus*, but which is displayed by medium-sized Late Miocene hyaenids from this basin, such as *Thalassictis*. We therefore remove IPS28746 from the hypodigm of *M. aphanistus* and attributed it to Hyaenidae indet. (see a discussion of the biostratigraphic implications below).

Can Mata: The talus from the classical collections of CM (IPS30901) shares several characters with those of *P. leo* (such as a moderately large neck, and a deep and mediolaterally compressed trochlea). In these features, this taxon differs from *Homotherium* and *Amphimachairodus*, which usually display a relatively shorter talar neck, together with a narrow and mediolaterally wide trochlea (Ballesio, 1963; Berta, 1987; Merriam and Stock, 1932; Salesa et al., 2012). The characters displayed by the studied talus therefore agree with the purported less derived morphology of *M. aphanistus* compared with both *Amphimachairodus* and *Homotherium*.

Can Poncic, Can Llobateres and Santiga: The remains of *Machairodus* from CP1, CLL1 and SA were published by Beaumont and Crusafont-Pairó (1982), who attributed them to *M.* cf. *aphanistus*. Here, we describe previously unpublished material from CLL1, mostly consisting of postcranial remains. The latter closely resemble in morphology the postcranial material of *M. aphanistus* from Los Valles de Fuentidueña (Crusafont-Pairó and Ginsburg, 1973), although the metacarpal shafts and the phalanges are stouter than in other machairodontins (more similar to the stoutly-built metacarpals and phalanges of *P. leo*).

La Tarumba and Viladecavalls: The felid material from LTR, in the area of Viladecavalls, was originally described and published by Villalta Comella and Crusafont Pairó (1943, 1948), who attributed it to *Felis antediluviana* and *Felis* sp. Villalta Comella and Crusafont Pairó (1943), in particular, reported from this locality a corpus fragment with p4–m1, whereas Villalta Comella and Crusafont Pairó (1948) reported a few postcranials (a second, third and fourth metacarpals, and a proximal phalanx) that they considered might belong to the same taxon recorded by the dentognathic fragment. The morphology of the right third metacarpal (IPS16286) is clearly that of a felid, and the proportions and morphology of the base allows us to include it in the hypodigm of *M. aphanistus* (Table 3), together with other postcranial specimens from the same locality. In contrast, the other metacarpals and the proximal phalanx described by Villalta Comella and Crusafont Pairó (1948) are mediolaterally wider and proximodistally shorter, which together with the morphology of the articular facets indicates an alternative attribution to an ursid, probably *Indarctos vireti*. In contrast, the mandibular fragment (IPS35093) described by Villalta Comella and

Crusafont Pairó (1943) is attributable to *Paramachaerodus* sp., on the basis of its shallow mandibular corpus, the presence of a well-developed accessory cuspids and a distinct buccal cingulid in the p4, and an m1 protoconid clearly longer mediodistally than the paraconid (J.M.-M. and J.M.R., unpublished data). Here, we also report a previously undescribed proximal phalanx (IPS36058) coming from an undeterminate stratigraphic horizon from the area of Viladecavalls. This specimen can be attributed to *M. aphanistus* based on similarities (robust shaft and deep ligamental groove) with the previously published material from Los Valles de Fuentidueña (Crusafont-Pairó and Ginsburg, 1973).

Ronda Oest Sabadell: The mandible from ROS-D3 is ascribed to *M. aphanistus* based on several characters displayed by material of this taxon from other Eurasian localities, such as Batallones-1 (Antón et al., 2004; Salesa et al., 2005; Turner et al., 2011), CLL1 (Beaumont and Crusafont-Pairó, 1982; this study), and Eppelsheim and Charmoille (Beaumont, 1975). According to the emended diagnosis of this species provided by Antón et al. (2004), these features include: large lower canines of oval cross-section; large lower premolars with a complete set of accessory cuspids; well-developed metaconid-talonid complex in m1; thick and high mandibular ramus; high and posteriorly inclined coronoid process; and undeveloped mandibular flange. The ROS specimen can be thus distinguished from *A. giganteus* by the possession of larger c1, the relatively broader p4, the non-reduced talonid-metaconid complex in the lower carnassial, and the poorly-developed flange. The specimen from ROS thus merely shows a few slight differences compared to the remains from other Eurasian localities, namely: relatively longer postcanine diastema; shorter p3 relative to p4 (Fig. 2E); better developed premolar accessory cuspids (especially in p4); and better developed m1 metaconid. *Amphimachairodus* displays several derived dental features relative to *Machairodus* (Geraads et al., 2004), which support the purported phyletic lineage constituted by the Vallesian *M. aphanistus*, the Turolian-Ventian *A. giganteus*, and the Plio-Pleistocene *Homotherium* (Kurtén and Anderson, 1980; Sotnikova, 1992). Dental evolution throughout this lineage would reflect the progressive acquisition of several traits already displayed to some degree by the Turolian-Ventian species (Geraads et al., 2004), including the reduced c1, shorter p3 (usually absent in *Homotherium*), larger p4 with a well-developed mesial accessory cuspid, and loss of the m1 talonid.

In the above-mentioned regards, the ROS specimen displays some derived traits compared to typical *M. aphanistus*, including the somewhat reduced p3 (Fig. 2A) and the longer postcanine diastema. Given that the ROS specimen fits with the known chronostratigraphic range of *M. aphanistus* from the Vallès-Penedès Basin and elsewhere in Eurasia, these slight differences support the view that the characters employed to distinguish Vallesian from Turolian-Ventian machairodontins are more variable than customarily recognized (Beaumont, 1975; Sotnikova, 1992), further including symphyseal height, development of the mandibular flange, length of the postcanine diastema, and relative size between the premolars. We therefore conclude that the above-mentioned slight dentognathic differences merely reflect the intraspecific variability of *M. aphanistus*. This is also supported by the fact that the ROS mandible still retains a well-developed p4 mesial accessory cuspulid as well as a distinct m1 talonid with a large metaconid (even larger than in typical *M. aphanistus*), which according to Geraads et al. (2004) should be interpreted as primitive features. Only a few complete mandibles of *M. aphanistus* are known from Eurasia, except from the large collection from Batallones, which in the future will hopefully enable a more complete assessment of intraspectific variability in this species.

Torrent de Febulines: The felid remains from TF were originally published by Golpe-Posse et al. (1979), who attributed the following remains to *M. aphanistus*: two C1 crown fragments (IPS28932), one scapholunar (IPS28932), a fifth metacarpal (IPS28904), a first metacarpal and an acetabulum fragment. The two latter specimens were not found among the ICP collections by the authors, and subsequently Pons-Moyà (1990), who restudied the *Machairodus* remains from TF, only described the remains that are reported here. According to Pons-Moyà (1990), these fossils should be attributed to *Amphimachairodus giganteus*, based on the buccolingual compression and crenulated morphology of the two canine fragments, as well as the morphological similarities of the fifth metatarsal with the material of this taxon from Concud (Pons-Moyà, 1990). Our assessment of the material indicates that the TF specimens display the same morphology as those from CLL1 and SA, merely differing from the latter by the slightly larger dimensions (and hence stouter appearance) of the former (Table 3). The scarce available material from TF thus lacks clear resemblances with *Amphimachairodus*, leading us to conclude that the above-mentioned differences in size compared to specimens of *M. aphanistus* from SA and CLL1 are merely attributable to the large degrees of interspecific variability and sexual dimorphism characteristic of medium to large-sized felids.

5.2. Locomotor inferences

M. aphanistus is mainly known on the basis of craniodental material, including several mandibles from various European sites and even complete skulls from Batallones-1 (Antón et al., 2004). In contrast, the postcranial anatomy of this early scimitar-toothed cat is practically unknown. Only scarce postcranial material was published by Crusafont-Pairó and Ginsburg (1973), Beaumont and Crusafont-Pairó (1982) and Pons-Moyà (1990), who nevertheless did not provide any inferences on the locomotor behavior of this species. The newly described postcranial remains of *M. aphanistus* (basically, carpals, metacarpals, tarsals, metatarsals and phalanges) allow us to provide important new data for better understanding the locomotor and predatory behavior of this taxon. The metacarpals and metatarsals are clearly stouter (mediolaterally wider) than in *Homotherium*, thus more closely resembling those of *P. leo* (Fig. 8; Ballesio, 1963; Rawn-Schatzinger, 1992). The proximodistally-elongated calcaneus, and the relatively long neck as well as deep and mediolaterally compressed trochlea of the talus are also more similar to those of

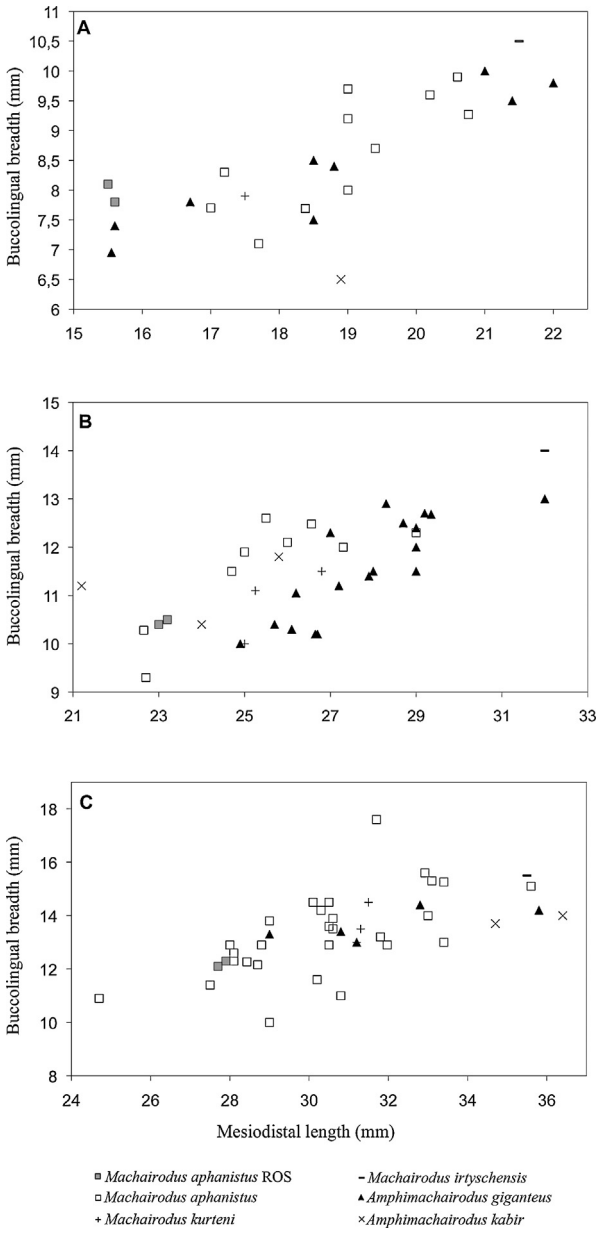

Fig. 7. Dental proportions of the lower cheek teeth in *Machairodus aphanistus* from ROS compared with other Late Miocene machairodontines. All points represent individual data, except for Batallones-1, where only the mean and the minimum–maximum ranges were available. **A**, p3; **B**, p4; **C**, m1.

Fig. 7. Proportions dentaires des prémolaires et molaires inférieures de *Machairodus aphanistus* de ROS, comparées avec celles d'autres machairodontinés du Miocène supérieur. Tous les points représentent les données individuelles, à l'exception de Batallones-1, où seule la moyenne et les intervalles minimum–maximum étaient disponibles. **A**, p3 ; **B**, p4 ; **C**, m1.

P. leo than to those of *Homotherium* (Ballesio, 1963; Rawn-Schatzinger, 1992). In contrast, the cuboid articular facets for the calcaneus and metatarsals are parallel, as in *Acinonyx* and *Homotherium*, instead of diverging as in *P. leo* (Ballesio, 1963; Hearst et al., 2011; Rawn-Schatzinger, 1992). The middle phalanges are proximodistally long, as in *P. leo*, rather than short as in *Homotherium*, but like those of the latter they display a lesser degree of mediolateral asymmetry than in *P. leo* (Ballesio, 1963; Hearst et al., 2011; Rawn-Schatzinger, 1992).

The long calcaneus and the morphology of talus (with a moderately long neck and a mediolaterally compressed and deep trochlea), similar to those of *P. leo*, indicate a digitigrade locomotion for *M. aphanistus* (Ballesio, 1963; Rawn-Schatzinger, 1992). In contrast, *Homotherium* displays a proximodistally short calcaneum and a bear-like talus with a proportionally short neck, these features being rather associated with a semiplantigrade stance with the ability to place the foot nearly flat on the ground (Ballesio, 1963; Rawn-Schatzinger, 1992).

The morphology of the studied cuboid and the lesser degree of asymmetry in the middle phalanges (which implies a smaller degree of claw retraction; Gonyea, 1976) resemble the condition seen in *H. serum* and *H. latidens* (Ballesio, 1963; Hearst et al., 2011; Rawn-Schatzinger, 1992). A smaller degree of claw retraction is usually related to the condition seen in *Acinonyx jubatus* and canids, which have non-retractile claws so as to combine high speed with catching ability (Rawn-Schatzinger, 1992). In the case of *Homotherium* and probably *M. aphanistus*, the lesser degree of asymmetry in the middle phalanges may be associated with a high degree of traction during hunting at high speeds (Ewer, 1973; Eaton, 1974; Rawn-Schatzinger, 1992).

Several authors have previously suggested long-distance travel capabilities in open habitats for *Homotherium* (Ballesio, 1963; Hearst et al., 2011; Rawn-Schatzinger, 1992). The detailed study of the postcranial remains of *Homotherium* shows that clearly cursorial features (the proportions of the hindlimbs and the non-retractile claws) are associated with more generalized terrestrial features (such as the morphology of the talus and calcaneum). This evidence suggests moderate cursorial abilities and a body plan adapted for running in *Homotherium* (Rawn-Schatzinger, 1992). In contrast, *M. aphanistus* appears as a more stoutly-built species that generally more closely resembles *P. leo*, including the morphology of the tarsal bones. This is evidenced, among other features, by the stoutness of the metapodials of *M. aphanistus*, which are mediolaterally much wider than in the more lightly-built *Homotherium*. The morphology of the middle phalanges, proximodistally long (as in *P. leo*) and with a low degree of asymmetry (resembling *Homotherium*), implies a moderate capacity of traction during hunting at high speeds, and foreshows to some degree the more derived traits displayed in this regard by *Homotherium* (Rawn-Schatzinger, 1992) Overall, thus, *M. aphanistus* displays several postcranial features more primitive than in *Homotherium*, with the former being apparently less adapted for long-distance travel and high-speed hunting than its putative descendant.

5.3. Biostratigraphy

Before this study, the earliest record of the genus *Machairodus* in the Vallès-Penedès Basin was thought to be in the early MN9 locality of CCN22, being slightly younger than the locality of CCN20, which records the first appearance datum of the equid *Hippotherium* in this basin, with

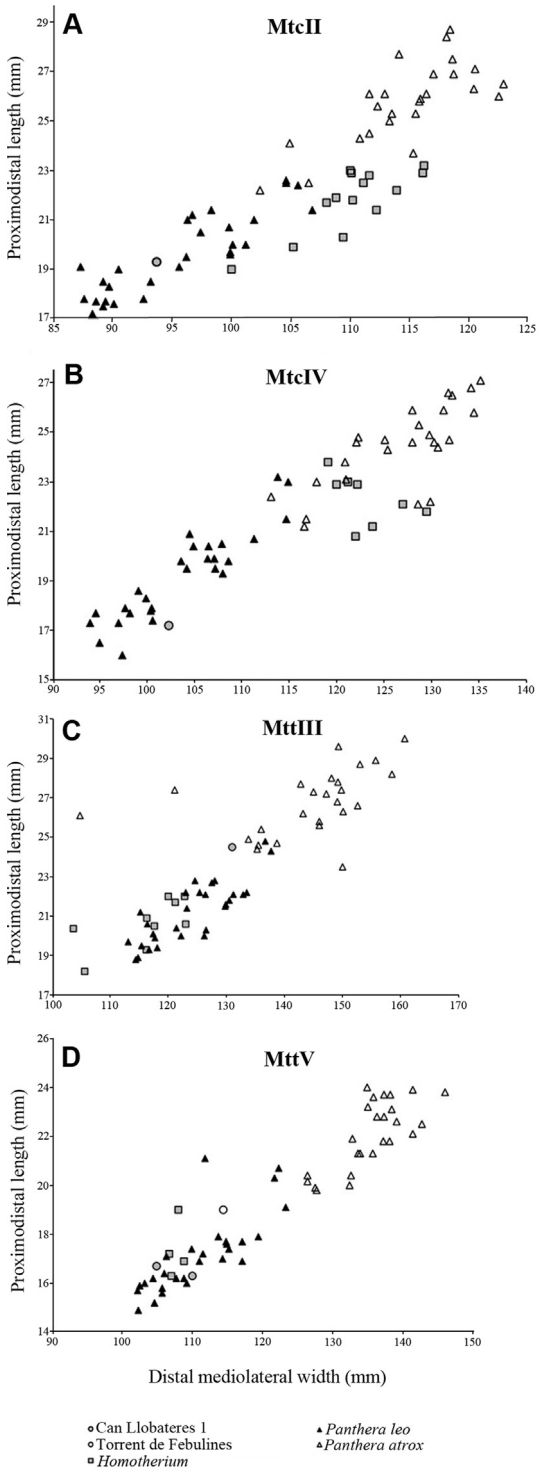

Fig. 8. Proportions of the metacarpals and metatarsals of *Machairodus aphanistus* from CLL and TF compared with those of other machairodontines and pantherines. **A**, Mtc II; **B**, Mtc IV; **C**, Mtt III; **D**, Mtt V.
Fig. 8. Proportions des métacarpiens et métatarsiens de *Machairodus aphanistus* de CLL et TF par rapport à celles d'autres machairodontinés et panthérinés. **A**, Mtc II ; **B**, Mtc IV ; **C**, Mtt III ; **D**, MttV.

an estimated age of 11.1 Ma (Agustí et al., 1997; Garcés et al., 1997). In fact, Agustí et al. (1997) considered that the putative joint dispersal of *Hippotherium* and *Machairodus* might be a major dispersal event of eastern immigrants, marking the beginning of "MN9a" (*Megacricetodon ibericus+Hippotherium* biozone). Agustí and Galobart (1998) reported the presence of *Machairodus* sp. from CCN20, although an inspection of the ICP collections showed that only a single carnivoran remain superficially resembling this taxon was available from locality CCN22, as reported by Agustí et al. (1997) and Casanovas-Vilar et al. (2006). Here, we show that this specimen belongs in fact to a hyaenid, indicating that the first appearance datum of *M. apahanistus* in the Vallès-Penedès might be younger than previously assumed.

On the other hand, the previously undescribed talus from CM described here probably represents the oldest Vallès-Penedès record of this genus. This specimen comes from the historical collections amassed decades ago by Miquel Crusafont et al. around Can Mata de la Garriga in els Hostalets de Pierola. This area records the Aragonian/Vallesian transition at 11.1 Ma (Alba et al., 2006, 2011b; Casanovas-Vilar et al., 2011a; Moyà-Solà et al., 2009), so that uncertainties concerning the precise stratigraphic horizon of provenance precludes determining with certainty whether the described talus is MN7+8 or MN9 in age. However, this specimen indicates at least that *M. aphanistus* was already recorded in this basin by the Earliest Vallesian. All the remaining Vallès-Penedès material of this taxon comes from younger localities, the oldest ones being CP1 and SA, with an estimated age comprised between 9.9 and 10.4 Ma (MN9). The new material from ROS-D3 (9.7–8.7 Ma, MN10), in contrast, is dated to the Late Vallesian, being probably coeval or slightly younger than that from LTR (ca. 9.6 Ma, MN10). However, the certain last occurrence datum of *M. aphanistus* in the Vallès-Penedès Basin corresponds to the site of TF (ca. 9.1 Ma, MN10). Overall, the chronostratigraphic range of *M. aphanistus* in the Vallès-Penedès Basin agrees with its known chronological distribution in the rest of Europe, where it is mainly recorded in MN9–MN10, with doubtful and scarce records in the Early Turolian (MN11) that might be alternatively attributable to *A. giganteus* (Antón et al., 2004).

6. Summary and conclusions

All the available craniodental and postcranial remains of the Late Miocene scimitar-toothed cat *M. aphanistus* from the Vallès-Penedès Basin are reviewed here, including previously unpublished material. The studied material comes from the following localities: Can Mata indeterminate (Late MN7+MN8 or MN9), Creu Conill 22 (MN9), Can Poncic 1 (MN9), Can Llobateres 1 (MN9), Santiga (MN9), La Tarumba 1 (MN10), Viladecavalls (MN10), Ronda Oest Sabadell ROS-D3 (MN10), and Torrent de Febulines (MN10). We show that the previously assumed oldest record of *M. aphanistus* in the Vallès-Penedès Basin, coming from Creu Conill 22 (11.1 Ma), corresponds in fact to a hyaenid, although based on the whole available sample the species is recorded from both MN9 and MN10. The postcranial remains described

in this paper suggest that *M. aphanistus* is a stoutly-built species, more closely resembling the extant *P. leo* instead of the more slender homotheriin *Homotherium*, which is customarily considered to have displayed a digitigrade locomotion with abilities for long-distance travel in open habitats. The more primitive postcranial morphology displayed by *M. aphanistus* suggests that this taxon was less adaptated for traveling long distances than its purported descendant *Homotherium*.

Acknowledgments

This work has been supported by the Spanish Ministerio de Ciencia e Innovación (CGL2011-28681, CGL2011-25754, CGL2010-21672, JCI-2010-08241 to ICV and RYC-2009-04533 to D.M.A.) and the Generalitat de Catalunya (2009 SGR 754 GRC). Fieldwork at Ronda Oest Sabadell was funded by UTE Ronda Oest and Gestió d'Infraestructures S.A.U., under the supervision of the Generalitat de Catalunya. The authors thank Jorge Morales and Mauricio Antón for discussions about the described fossil material, Eli Blaya for processing data from ROS, and Salvador Moyà-Solà for various kinds of support. Careful reading and thoughtful comment by two anonymous reviewers greatly improved the manuscript.

References

Abella, J., Domingo, M.S., Valenciano, A., Montoya, P., Morales, J., 2011. La asociación de carnívoros de Batallones 3, Mioceno superior del Cerro de los Batallones Cuenca de Madrid. Paleontol. Evol. memòria especial núm. 5, 21–24.

Agustí, J., Moyà-Solà, A., Gibert, J., 1984. Mammal distribution dynamics in the eastern margin of the Iberian Peninsula during the Miocene. Paléobiol. Contin. 14, 33–46.

Agustí, J., Cabrera, L., Moyà-Solà, S., 1985. Sinopsis estratigráfica del Neógeno de la fosa del Vallès-Penedès. Paleontol. Evol. 18, 57–81.

Agustí, J., Cabrera, Ll., Garcés, M., Parés, J.M., 1997. The Vallesian mammal succession in the Vallès-Penedès basin (Northeast Spain): paleomagnetic calibration and correlation with global events. Palaeogeogr. Palaeoclimatol. Palaeoecol. 133, 149–180.

Alba, D.M., Moyà-Solà, S., Casanovas-Vilar, I., Galindo, J., Robles, J.M., Rotgers, C., Furió, M., Angelone, C., Köhler, M., Garcés, M., Cabrera, L., Almécija, S., Obradó, P., 2006. Los vertebrados fósiles del Abocador de Can Mata (els Hostalets de Pierola, Anoia, Cataluña), una sucesión de localidades del Aragoniense superior (MN6 y MN7+8) de la cuenca del Vallès-Penedès. Estudios Geol. 62, 295–312.

Alba, D.M., Casanovas-Vilar, I., Moyà-Solà, S., Robles, J.M., 2011a. Parada 4 El Vallesiense inferior y su transición con el Vallesiense superior: Can Llobateres. Paleontol. Evol. memòria especial núm. 6, 111–123.

Alba, D.M., Casanovas-Vilar, I., Robles, J.M., Moyà-Solà, S., 2011b. Parada 3 El Aragoniense superior y la transición con el Vallesiense: Can Mata y la exposición paleontological de els Hostalets de Pierola. Paleontol. Evol. Memòria especial núm. 6, 95–109.

Antón, M., Salesa, M.J., Morales, J., Turner, A., 2004. First known complete skulls of the scimitar-toothed cat *Machairodus aphanistus* (Felidae Carnivora) from the Spanish Late Miocene site of Cerro Batallones-1. J. Vert. Paleontol. 24, 957–969.

Antón, M., Salesa, M.J., Siliceo, G., 2013. Machairodont adaptations and affinities of the Holarctic Late Miocene homotherin *Machairodus* (Mammalia, Carnivora Felidae): The case of *Machairodus catocopis* Cope, 1887. J. Vert. Paleontol. 33, 1202–1213.

Ballesio, R., 1963. Monographie d'un *Machairodus* du gisement villafranchien de Senèze : *Homotherium crenatidens Fabrini*. Trav. Lab. Géol. Fac. Sci. Lyon 9, 1–127.

Bartrina, M.T., Cabrera, L., Jurado, M.J., Guimerà, J., Roca, E., 1992. Evolution of the central Catalan margin of the Valencia trough (western Mediterranean). Tectonophysics 203, 219–247.

Beaumont, G., 1975. Recherches sur les Félidés (Mammifères Carnivores) du Pliocène inférieur des sables à *Dinotherium* des environs d'Eppelsheim. Arch. Sci. 28, 369–405.

Beaumont, G., Crusafont-Pairó, M., 1982. Les Félidés (Mammifères, Carnivores) du Vallésien du Vallès, Catalogne, Espagne. Arch. Sci. 35, 41–64.

Bernor, R.L., Kovar-Eder, J., Lipscomb, D., Rögl, F., Sen, S., Tobien, H., 1988. Systematic, stratigraphic and palaeoenvironmental contexts of first-appearing *Hipparion* in the Vienna basin, Austria. J. Vert. Paleontol. 8, 427–452.

Berta, A., 1987. The sabercat *Smilodon gracilis* from Florida and a discussion of its relationships (Mammalia, Felidae Smilodontine). Bull. Fla. Mus. Nat. Hist. Biol. Sci. 31, 1–63.

Blaya Martí, E., Obradó, P., Robles, J.M., Sala, J., Alba, D.M., 2012. Memòria de la intervenció paleontològica preventiva a les obres de prolongació de la Ronda Oest Sabadell tram comprès entre la carretera N-150 i la BV-1248 (Sabadell, el Vallès Occidental): 2008–2011. FOSSILIA Serveis Paleontològics i Geològics SL (unpublished report).

Bonis, L. de, 1994. Des gisements de Mammifères du Miocène supérieur de Kemiklitepe, Turquie. 2. Bull. Mus. Natl. Hist. Nat. 16, 19–39.

Cabrera, L., Calvet, F., Guimerà, J., Permanyer, A., 1991. El registro sedimentario miocénico en los semigrabens del Vallès-Penedès y de El Camp: organización secuencial y relaciones tectónican-sedimentación. I Congreso Grupo Español del Terciario. In: Libro-Guía Excursión 4 (132 p. Vic).

Cabrera, L., Roca, E., Garcés, M., de Porta, J., 2004. Estratigrafía y evolución tectonosedimentaria oligocena superior-neógena del sector central del margen catalán (Cadena Costero-Catalana). In: Vera, J.A. (Ed.), Geología de España. SGE-IGME, Madrid, pp. 569–573.

Casanovas-Vilar, I., Furió, M., Agustí, J., 2006. Rodents, insectivores and paleoenvironment associated to the first-appearing hipparionine horses in the Vallès-Penedès Basin (northeastern Spain). Beitr. Paläont. 30, 89–107.

Casanovas-Vilar, I., Alba, D.M., Garcés, M., Robles, J.M., Moyà-Solà, S., 2011a. Updated chronology for the Miocene hominoid radiation in western Eurasia. Proc. Natl. Acad. Sci. U S A 108, 5554–5559.

Casanovas-Vilar, I., Alba, D.M., Robles, J.M., Moyà-Solà, S., 2011b. Registro paleontológico continental del Mioceno de la cuenca del Vallès-Penedès. Paleontol. Evol. memòria especial 6, 55–80.

Christiansen, P., Adolfssen, J.S., 2007. Osteology and ecology of *Megantereon cultridens* [311SE] (Mammalia; Felidae; Machairodontinae), a sabrecat from the Late Pliocene and Early Pleistocene of Senéze, France. Zool. J. Linn. Soc. Lond. 151, 833–883.

Crusafont, M., Truyols, J., 1954. Catálogo paleomastológico del Mioceno del Vallés-Penedés y de Calatayud-Teruel. Segundo Cursillo Internacional de Paleontología. Museu de la Ciudad de Sabadell, Sabadell.

Crusafont Pairó, M., 1959. Primer hallazgo en España del género *Ursavus* (Carnivora Ursidae). Not. Com. Inst. Geol. Min. Esp. 55, 137–144.

Crusafont Pairó, M., 1964. La biota de Can Llobateres (Sabadell) y su significación biológica. Curs. Conf. Inst. "Lucas Mallada" 9, 177–179.

Crusafont-Pairó, M., Golpe-Posse, J.M., 1972. New Pongids from the Miocene of the Vallès Penedes Basin (Catalonia, Spain). J. Hum. Evol. 2, 17–23.

Crusafont-Pairó, M., Ginsburg, L., 1973. Les Carnassiers fossiles de Los Vallès de Fuentidueña (Ségovie, Espagne). Bull. Mus. Natl. Hist. Nat. 131, 29–45.

Crusafont Pairó, M., Kurtén, B., 1976. Bears and bear-dogs from the Vallesian of the Vallès-Penedès Basin, Spain. Acta Zool. Fenn. 144, 1–29.

de Gibert, J.M., Casanovas-Vilar, I., 2011. Contexto geológico del Mioceno de la cuenca del Vallès-Penedès. Paleontol. Evol. memòria especial 6, 39–45.

Eaton, R.L., 1974. The Cheetah: the biology, ecology and behaviour of an endangered species. Van Nostrand Reinhold Co., New York (178 p.).

Ewer, R.F., 1973. The carnivores. Cornell. University Press, New York (494 p.).

Fraile, S., Pérez, B., De Miguel, I., Morales, J., 1997. Revisión de los carnívoros presentes en los yacimientos del Neógeno español. In: Calvo, J.P., Morales, J. (Eds.), Avances en el conocimiento del Terciario ibérico. , pp. 77–80.

Garcés, M., Agustí, J., Cabrera, L., Parés, J.M., 1996. Magnetostratigraphy of the Vallesian (Late Miocene) in the Vallès-Penedès Basin (Northeast Spain). Earth Planet. Sci. Lett. 142, 381–396.

Garcés, M., Cabrera, L., Agustí, J., Parés, J.M., 1997. Old World first appearance datum of "*Hipparion*" horses: Late Miocene large-mammal dispersal and global events. Geology 25, 19–22.

Gaudry, A., 1832. Animaux fossiles et géologie de l'Attique. F. Savy, Paris (475p.).

Geraads, D., 1989. Vertébrés fossiles du Miocène supérieur du Djebel Krechem el Artsouma (Tunisie centrale). Comparaisons biostratigraphiques. Geobios 22, 777–801.

Geraads, D., Alemseged, Z., Bellon, H., 2002. The Late Miocene mammalian fauna of Chorora Awash basin, Ethiopia: systematics, biochronology and the ^{40}K-^{40}Ar ages of the associated volcanics. Tertiar. Res. 21, 113–122.

Geraads, D., Kaya, T., Tuna, V., 2004. A skull of *Machairodus giganteus* (Felidae Mammalia) from the Late Miocene of Turkey. N. Jb. Geol. Paläont. Mon. 2, 95–110.

Ginsburg, L., Morales, J., Soria, D., 1981. Nuevos datos sobre los carnívoros de los Valles de Fuentidueña (Segovia). Estudios Geolog. 37, 383–415.

Golpe-Posse, J.M., 1974. Faunas y yacimientos con suiformes del Terciario español. Paleontol. Evol. 8, 1–87.

Golpe Posse, J.M., Santafe, L., Lopis, J.V., Casanovas, C., 1979. Datos sobre el Vallesiense medio-superior de los alrededores de Terrassa. Acta Geol. Hisp. 14, 356–361.

Gonyea, W.J., 1976. Behavioral implications of saber-toothed felid morphology. Paleobiol. 2, 332–342.

Hearst, J.M., Martin, L.D., Babiarz, J.P., Naples, V.L., 2011. Osteology and myology of *Homotherium ischyrus* from Idaho. In: Naples, V.L., Martin, L.D., Babiarz, J.P. (Eds.), The Other Saber-tooths: Scimitar-tooth Cats of the Western Hemisphere. The John Hopkins University Press, Baltimore, pp. 123–183.

Kurtén, B., 1976. Fossil Carnivora from the Late Tertiary of Bled Douarah and Cherichira. Tunisia. Not. Serv. Geol. Tunisie 42, 177–214.

Kurtén, B., Anderson, E., 1980. Pleistocene Mammals of North America. Columbia University Press, New York.

Martin, L.D., 1998. Felidae. In: Janis, C.J., Scott, K.M., Jacobs, L.L. (Eds.), Evolution of Tertiary Mammals of North America, Vol. 1. Terrestrial Carnivores, Ungulates and Ungulate like Mammals, Cambridge University Press, Cambridge, pp. 144–151.

Martin, L.D., Naples, V.L., Babiarz, J.P., 2011. Revision of the new World Homotheriini. In: Naples, V.L., Martin, L.D., Babiarz, J.P. (Eds.), The Other Saber-tooths: Scimitar-tooth Cats of the Western Hemisphere. The John Hopkins University Press, Baltimore, pp. 185–194.

Mein, P., 1999. The Late Miocene small mammal succession from France, with emphasis on the Rhône Valley localities. In: Agustí, J., Rook, L., Andrews, P. (Eds.), Hominoid Evolution and Climatic Change in Europe. Vol. 1. The Evolution of Neogene Terrestrial Ecosystems in Europe. Cambridge University Press, Cambridge, pp. 140–164.

Merriam, J.C., Stock, C., 1932. The Felidae of Rancho la Brea. No. 422. Carnegie Institution of Washington, Washington.

Montoya, P., Morales, J., Robles, F., Abella, J., Benavent, J.V., Marín, M.D., Ruiz Sánchez, F.J., 2006. Las nuevas excavaciones (1995–2006) en el yacimiento del Mioceno final de Venta del Moro, Valencia. Estudios Geol. 62, 316–326.

Morales, J., Pozo, M., Silva, P.G., Domingo, M.S., López-Antoñanzas, R., Álvarez Sierra, M.A., Antón, M., Martín Escorza, C., Quiralte, V., Salesa, M.J., Sánchez, I.M., Azanza, B., Calvo, J.P., Carrasco, P., García-Paredes, I., Knoll, F., Hernández Fernández, M., van den Hoek Ostende, L., Merino, L., van der Meulen, A., Montoya, P., Peigné, S., Peláez-Campomanes, P., Sánchez Marco, A., Turner, A., Abella, J., Alcalde, G.M., Andrés, M., DeMiguel, D., Cantalapiedra, J.L., Fraile, S., García Yelo, B.A., Gómez Cano, A.R., López Guerrero, P., Oliver Pérez, A., Siliceo, G., 2008. El sistema de yacimientos de mamíferos miocenos del Cerro de los Batallones Cuenca de Madrid: estado actual y perspectivas. Palaeontol Nova Publ. Sem. Paleontol. Zaragoza. 8, 41–117.

Morlo, M., 1997. Die Raubtiere (Mammalia, Carnivora) aus dem Turolium von Dorn-Dürkheim 1 (Rheinhessen). Teil 1: Mustelida, Hyaenidae, Percrocutidae Felidae. Cour. Forsch. -Inst. Senckenberg 197, 11–47.

Moyà-Solà, S., Köhler, M., Alba, D.M., Casanovas-Vilar, I., Galindo, J., Robles, J.M., Cabrera, L., Garcés, M., Almécija, S., Beamud, E., 2009. First partial face and upper dentition of the Middle Miocene hominoid *Dryopithecus fontani* from Abocador de Can Mata (Vallès-Penedès Basin, Catalonia, NE Spain): taxonomic and phylogenetic implications. Am. J. Phys. Anthropol. 139, 126–145.

Orlov, Y.A., 1936. Tertiäre Raubtiere des Westlichen Sibiriens I. Machairodontinae. Trav. Inst. Paleozool. Acad. Sci. URSS 5, 111–152.

Peigné, S., Bonis, L., de, Likius, A., Mackaye, H.T., Vignaud, P., Brunet, M., 2005. A new Machairodontine (Carnivora, Felidae) from the Late Miocene hominid locality of TM66, Toros-Menalla, Chad. C. R. Palevol. 4, 243–253.

Pons-Moyà, J., 1990. Presencia de carnívoros turolienses en el Vallesiense terminal (MN 10) de Terrassa (Catalunya). Paleontol. Evol. 23, 199–203.

Qiu, Z.-X., Shi, Q.-Q., Liu, J.-Y., 2008. Description of skull material of *Machairodus horribilis* Schlosser, 1903. Vert. Pal. Asiat. 46, 265–283.

Roca, E., Guimerà, J., 1992. The Neogene structure of the eastern Iberian margin: structural constraints on the crustal evolution of the Valencia Trough (western Mediterranean). Tectonophysics 203, 203–218.

Rawn-Schatzinger, V., 1992. The scimitar cat *Homotherium serum*. Cope. ISM Rep. Invest. 47, 1–80.

Salesa, M.J., Antón, M., Morales, J., 2005. Inferred behaviour and ecology of the primitive sabre-toothed cat *Paramachairodus ogygia* (Felidae Machairodontinae) from the Late Miocene of Spain. J. Zool. 268, 243–254.

Salesa, M.J., Pesquero, M.D., Siliceo, G., Antón, M., Alcalá, L., Morales, J., 2012. A rich community of Felidae (Mammalia, Carnivora) from the Late Miocene (Turolian, MN13) site of Las Casiones (Villalba Baja, Teruel, Spain). J. Vert. Paleontol. 32, 658–676.

Sardella, R., Werdelin, L., 2007. *Amphimachairodus* (Felidae, Mammalia) from Sahabi (Latest Miocene–Earliest Pliocene, Libya), with a review of African Miocene Machairodontinae. Riv. Ital. Paleontol. Stratigr. 113, 67–77.

Sotnikova, M.V., 1992. A new species of *Machairodus* from the Late Miocene Kalmakpai locality in eastern Kazakhstan (USSR). Ann. Zool. Fennici 28, 361–369.

Spassov, N., Tzankov, Tz., Geraads, D., 2006. Late Neogene stratigraphy, biochronology, faunal diversity and environments of south-western Bulgaria. Geodiversitas 28, 477–498.

Turner, A., Antón, M., Salesa, M.J., Morales, J., 2011. Changing ideas about the evolution and functional morphology of Machairodontine felids. Estudios Geol. 67, 255–276.

Van Dam, J.A., Alcalá, L., Alonso-Zarza, A., Calvo, J.P., Garcés, M., Krijgsman, W., 2001. The Upper Miocene mammal record from the Teruel-Alfambra region (Spain). The MN system and continental stage/age concepts discussed. J. Vert. Paleontol. 21, 367–385.

Villalta Comella, de J.F., Crusafont Pairó, M., 1943. Los vertebrados del Mioceno continental de la cuenca del Vallés-Panadés (provincia de Barcelona) I. Insectívoros. II. Carnívoros. Bol. Inst. Geol. Min. Esp. 56, 145–331.

Villalta Comella, de J.F., Crusafont Pairó, M., 1948. Nuevas aportaciones al conocimiento de los carnívoros pontienses del Vallés-Penedés. Miscelánea Almera. Publicaciones del Instituto Geológico 7, 81–121.

Werdelin, L., 2003. Mio-Pliocene Carnivora from Lothagam, Kenya. In: Leakey, M.G., Harris, J.M. (Eds.), Lothagam: the Dawn of Humanity in Eastern Africa. Columbia University Press, New York, pp. 261–328.

Werdelin, L., Sardella, R., 2006. The "*Homotherium*" from Langebaanweg, South Africa, and the origin of *Homotherium*. Palaeontogr. Abt. A. 277, 123–130.

Werdelin, L., Peigné, S., 2010. Carnivora. In: Werdelin, L., Sanders, W.J. (Eds.), Cenozoic Mammals of Africa. University of California Press, Berkeley, CA, USA, pp. 603–657.